OBSERVATIONS OF THE STRUCTURE OF RADIO SOURCES IN THE 3C CATALOGUE—II

C. D. Mackay

(Communicated by M. Ryle)

SUMMARY

The One-Mile radio telescope at Cambridge has been used to map the structure of a further 60 radio sources in the 3C catalogue at 408 MHz and 1407 MHz. This paper presents contour maps of the sources together with a list giving the position, angular size and flux density of each component; the optical fields of the same regions of sky are also briefly described.

1. INTRODUCTION

One of the main observing programmes of the One-Mile Radio Telescope at Cambridge (**1**) has been the determination of the structure of a large sample of extragalactic radio sources. Maps of 82 sources in the 3C catalogue have already been published (**2**), referred to hereafter as Paper I. The present paper gives the results for a further 60 sources. The sources in these two papers, together with a list of 78 unresolved or just resolved sources now being prepared by Elsmore and Mackay, include all those in the Revised 3C catalogue ($S_{178} \geqslant 9 \times 10^{-26}\,\mathrm{W\,m^{-2}\,Hz^{-1}}$) with $\delta > +10°$ and $|b^{\mathrm{II}}| > 10°$, thus providing a complete homogeneous sample as a basis for a number of theoretical investigations (**3**). The present paper includes the results for a few sources outside this sample.

Since the methods used in the observation and reduction of the data and the manner of presentation of the results follow closely those of Paper I, only a short description will be given here. The observations are described in Section 2, and the results are given in Section 3. Data for each source are given in Table II, with maps in Figs. 1–20. A number of the sources are identified with optical objects, and for these a distance has been estimated, and a number of physical parameters derived (Table III).

2. THE OBSERVATIONS

The One-Mile telescope was used to make observations simultaneously at two frequencies, 408 MHz and 1407 MHz, giving pencil beam responses whose widths between half-power points in right ascension are, respectively, about 80″ and 23″ arc. For the observation of sources which occupy only a small part of the envelope pattern it is not necessary to make observations at every spacing and a circular grating instrument may be synthesized with a much shorter observing time (**1**).

The telescope consists of three 18 m dishes, two fixed and one moveable, in an East–West line, which are connected as phase-switching interferometers giving two aerial spacings simultaneously. All aerial spacings up to 1·5 km are possible, and

by setting the dishes to follow a source over the sky for a 12-hour period the instrument is able to sample the Fourier transform of the sky brightness distribution at every point on two circular rings in a plane parallel to the equator. This is repeated for different aerial separations at intervals of a up to a maximum of D ($= Na$). Fourier inversion of the data gives a map of the source. For sources at high declinations, the reception pattern consists of a main response of width $\sim \lambda/D$ surrounded by grating ring responses of radius $\sim n\lambda/a$ for the nth ring. At other declinations, the reception pattern is broadened in declination by cosec δ. For a particular source the interval a is chosen so that the radius of the innermost grating ring ($\sim \lambda/a$) exceeds the total angular extent of the source.

When a source is observed for the first time with the instrument, nothing is assumed about the total angular extent of the source; observations over a 12-hour period with the maximum possible aerial spacings (D and $D/2$, where $D = 1502$ m), provide the amplitude A and phase relative to some reference point near the centre of the source $\varphi - \varphi_0$ (**1**). The range of frequencies present in the 12-hour plots of A and $\varphi - \varphi_0$ indicates the total angular extent of the bright regions of the source, and, hence, the value of a and the number of additional 12-hour observations needed.

The choice of a determines an upper limit of $\sim 0\cdot5\ \lambda/a$ to the scale of the angular structure that can be detected with the instrument. This is equivalent to $0'\cdot22 \times N$ and $0'\cdot75 \times N$ at the two observing frequencies of 1407 MHz and 408 MHz. For observations at a single frequency the existence of an extensive 'halo' of low surface brightness and containing no fine angular structure could be missed if its angular diameter exceeded $0\cdot5\ \lambda/a$; since, however, the interval a is chosen for the 1407 MHz observations, the presence of such a halo would be revealed by the simultaneous observations at 408 MHz unless the diameter of the halo was more than three times greater than the maximum extent of any other structure in the source. In addition, the total flux density derived from the maps was compared with that obtained with instruments of much lower resolving power. The spectra of all sources in the 3C catalogue have now been investigated in some detail (**4**) and the intregrated flux densities at 408 MHz and 1407 MHz are known with good accuracy. By comparing these values with the integrated flux density found in the present observations, it was usually possible to set an upper limit of better than 10 per cent to the flux density due to a possible halo; even if spectral differences between the halo and main components exist, the observations are unlikely to miss any features having a surface brightness greater than 2 per cent of the main components.

In the case of the few sources where there was evidence for an extended component of low surface brightness, additional observations were made at small aerial spacings and the results are described in the notes on individual sources.

For the two very extended sources, 3C 326 and 3C 442, it was more economical of observing time to arrange that the source lay within the first grating response at 408 MHz only; information on the fine structure of these sources may still be obtained from the observations at 1407 MHz. One source, 3C 435·1, was found to consist of three relatively compact components, and a value of a was chosen that was adequate for mapping the structure of individual components, although the rings from the different components intersected. In the case of 3C 35, components not present on the 1407 MHz map were found at 408 MHz which lie within and on the first grating response. Only a sketch map of the source is given at 408 MHz.

During these observations a number of sources were observed which were only just resolved at the maximum spacing at 1407 MHz. Information on their angular structure was more conveniently obtained from the 12-hour plots of A and $\varphi - \varphi_0$, and the results are described by Elsmore and Mackay.

As in Paper I, the scale of flux density was based upon the following values for the calibration sources used (Williams, private communication) which are believed to be accurate to within about 5 per cent.

TABLE I

Source	Flux density (10^{-26} W m^{-2} Hz^{-1})	
	408 MHz	1407 MHz
3C 48	35	15·5
147	47	22·5
196	37	15·0
295	48·5	23·0

3. PRESENTATION OF THE RESULTS

(a) *Contour Maps*

Maps of the sources are given in Figs. 1–20, approximately in order of increasing 3C number; they are derived from the 1407 MHz observations, except for a few sources of large extent where the 408 MHz maps are given.

The maps have all been drawn with the declination scale contracted by sin δ so that the beam of the instrument appears circular. An L-shape with arms 20″ arc long in the sky, has been drawn on each map to indicate the extent of this compression of the declination scale. In order to produce the minimum side-lobe response within the first grating ring, a slightly different aperture grading is used in maps derived from only two spacings; the half-power width of the synthesized beam is 20″ arc for these maps but for all other maps the width is 23″ arc. The maps are drawn on a standard scale which is three times greater at 1407 MHz than at 408 MHz.

1950·0 coordinates are used throughout.

The contour interval used depends on the flux density and extent of the individual source so that as much information as possible may be given without the maps becoming obscure. Because the zero-order spacing of the synthesis is omitted, the zero level on the maps is arbitrary. The choice of starting level for the full contours may differ by up to half a contour interval from the zero level. The total flux density is derived from the plots of A from the 12-hour observation at the smallest spacing. Map integration is used in deriving the relative flux densities of individual features, but the uncertainty in zero level does not generally introduce an appreciable error. For sources in which there are extensive features of low surface brightness, additional contours at half the normal interval are included; these are shown by thin lines on the maps. Negative contours, due to side-lobe responses, are shown by dotted lines.

For every source the prints of the National Geographic–Palomar Sky Survey were examined and the positions of optical objects that may be related are marked on the maps. Where possible, the accurate measurements of position by Griffin (5) and Véron (6) have been used. In other cases, the positions have been measured from the Sky Survey prints using a transparent overlay procedure similar to that

3

described by Longair (**7**), which gives a positional accuracy of about $\pm 5''$ arc and some indication of the colour of the object.

Photometric measurements of the apparent magnitude have been used where available. In some cases, the estimates of Longair (**7**) and Wyndham (**8, 9**) are quoted; for other sources, the magnitude was estimated from the prints. These estimates are believed to be accurate to within about one magnitude. The magnitudes given are the photovisual magnitude m_v, unless the photoelectric V magnitude is known; it is then indicated by '$V =$'.

Details of the optical objects marked on the maps are given in the figure captions; the following abbreviations have been used for references which occur particularly frequently.

G	(**5**)	Griffin
L	(**7**)	Longair
MMS	(**10**)	Matthews, Morgan & Schmidt
S	(**11**)	Schmidt
SVW	(**12**)	Sandage, Véron & Wyndham
V	(**6**)	Véron
W1	(**8**)	Wyndham 1965
W2	(**9**)	Wyndham 1966
WP	(**13**)	Wills & Parker

(b) *Source List*

The columns in Table II give the following information.

(1) The number of the source in the 3C catalogue (**14**), revised by Bennett (**15**). Sources marked * are not included in the revised catalogue. If the entry 'at 408 MHz' occurs, then the structural data were obtained at that frequency, and not at 1407 MHz as is otherwise the case.

(2) Morphological classification of the radio structure, according to the following scheme, which is the same as that adopted in Paper I.

A   Symmetrical single peaked extended source. The size is specified by total angular half-power widths along major and minor axes ($\omega_{\parallel}$ and $\omega_{\perp}$ see Column 8). The angular half-power widths are obtained from the maps on the assumption that the source has a Gaussian brightness distribution, with a correction for beam broadening. If a source does not have a Gaussian brightness distribution, the angular sizes given can only be a rough indication of the size of the source; for example, if it consists of two unresolved components of equal flux density, with an angular separation of $10''$ arc, the half-power width would be measured to be $12''\cdot8$ arc. When only an upper limit is given for $\omega_{\perp}$ the source was unresolved at right angles to its major axis.

AB   Single peaked extended source whose structure could be attributed to a moderately close unequal double source. The angular size is specified by the separation of the components (θ, see Column 6). For sources which are not extended enough to allow an unambiguous value of θ to be given, the size is specified by $\omega_{\parallel}$ as in type A.

ABb   Single peaked extended source which cannot be due simply to two unresolved components. For these sources θ gives the total angular extent and $\omega_{\parallel}$ and $\omega_{\perp}$ the size of the main peak.

B   Double source.

Bb, B(b)   Double source with a bridge of emission between the components; the brackets denote the bridge is doubtful.

BC   Double source with complex structure in the components.

C   Complex or multiple source.

(3) The number N of interferometric spacings used. The spacing intervals at 408 MHz and 1407 MHz are $2039/N$ and $7047/N$ wavelengths respectively; the maps contain all the structure on a scale not greater than $0'\!\cdot\!75 \times N$ and $0'\!\cdot\!22 \times N$ respectively.

(4) The sense of polarization observed. The observations are made with linear polarization. For sources denoted ' 1 ' the position angle of the electric vector is $0°$ at 1407 MHz and $90°$ at 408 MHz; for sources denoted ' 2 ' the reverse is true. For eight sources, denoted ' 12 ', a mixture of both senses of observation was used; as the percentage of polarized emission from most sources is small at 1407 MHz there should be little error in the maps made this way.

(5) The right ascension and declination of the peaks of emission at 1407 MHz with standard errors.

(6) Total angular size, θ. For simple double sources, θ is the separation between the peaks given in Column 5; for BC sources θ gives the separation between extreme peaks. For single peaked sources in classes AB and ABb, and for complex sources, θ is the overall angular extent measured from the map and corrected for beam broadening. For Class A and some Class AB sources, θ has been omitted, and the size specified by $\omega_\parallel$ and $\omega_\perp$ in Column 8.

(7) The position angle of the main radio axis; this is not, in general, the apparent position angle on the map because of the compression of the declination scale. For complex sources such as 3C 315, no value is given.

(8) The angular size of the components at 1407 MHz, being measured along the line of p.a. given in Column 7 and at right angles to it; for the more complex sources measurements were made along the major and minor axes of each component. For small sources and components, the values of $\omega_\parallel$ and $\omega_\perp$ quoted are found by fitting Gaussian models to the interferometer amplitude plots, and giving the corresponding half-power widths as described above.

(9) Peak brightness temperatures at 1407 MHz, in degrees Kelvin.

(10) Values of flux density with estimated errors at the two observing frequencies, on the assumption that the sources are unpolarized. For well extended sources, the relative fluxes from different regions of the source have been derived from the maps; for all sources the total flux densities have been obtained directly from the plots of interferometer amplitude.

(11) Spectral index α derived from the present observations at 408 MHz and 1407 MHz, defined in the sense $S \propto \nu^{-\alpha}$; it is given only for those sources which are resolved into separate components at both frequencies.

(12) Optical identifications; doubtful identifications are enclosed in brackets.

(13) References.

Notes on individual sources in Table II

3C 28. There is a weak source at $\alpha = 00^h 53^m 21^s\!\cdot\!50 \pm 0^s\!\cdot\!4$, $\delta = 26° 11' 07'' \pm 5''$ to the North-East of the main source contributing about 18 per cent of the total

TABLE II

The Source List

Position (1950.0)

Source number	Type	N	Poln	R.A. h	m	s	±s	Dec. °	′	″	±″	θ (″)	p.a. (°)	$\omega_\parallel$ (″)	$\omega_\perp$ (″)
3C 28	A	4	2	00	53	08.65	0.2	26	08	25.9	3	—	146	29	<11
35	C	4	2	01	08	55.8	1.2	49	08	31.5	15	560	14	~126	~40
(at				01	09	03.1	1.5	49	11	27.1	20			—	—
408 MHz)				01	09	09.1	1.5	49	17	26.5	20			~120	~45
41	AB	4	1	01	23	54.91	0.1	32	57	42.7	3	—	146	26	<10
42	AB	4	2	01	25	43.08	0.3	28	47	31.7	4	~25	132	—	<12
44	BC	4	12	01	28	44.72	0.2	06	08	16	15	880	4	—	—
				01	28	50.92	1.0	06	22	48	60			—	—
65	AB	2	1	02	20	36.79	0.2	39	47	19.9	2	—	104	17	<11
68.1	B	4	2	02	29	26.98	0.1	34	10	57.5	2	58	173	<13	<7
				02	29	27.19	0.5	34	10	00	8			<13	<10
98	BC	8	2	03	56	07.03	0.2	10	15	24.1	12	310	25	~76	~34
				03	56	14.18	0.2	10	19	10.5	12			~60	~26
111	C	8	2	04	14	54.92	0.2	37	53	34.9	3	198	~60	~11	<14
				04	15	00.48	0.2	37	54	20.5	3			~11	~14
				04	15	04.01	0.4	37	54	47.7	4			—	—
				04	15	09.34	0.2	37	55	14.2	3			15	<14
123	AB	4	1	04	33	55.71	0.4	29	34	08.1	5	—	152	29	9
132	AB	2	2	04	53	42.37	0.1	22	44	42.4	5	—	132	16	<14
133	AB	2	2	04	59	54.35	0.1	25	12	11.6	4	—	94	13	<16
169.1	B	4	2	06	47	34.65	0.2	45	13	16.9	3	38	137	~9	~9
				06	47	37.14	0.2	45	12	49.0	3			<8	<8
172	B	4	2	06	59	03.15	0.2	25	17	28.4	3	86	15	<15	<7
				06	59	04.85	0.2	25	18	51.6	3			~16	8
175	B	8	2	07	10	13.83	0.2	11	51	09.6	10	48	52	<26	<26
				07	10	16.41	0.2	11	51	33.0	10			<26	<26
192	C	8	2	08	02	29.46	0.3	24	19	23.5	6	209	123	20	<16
				08	02	32.68	0.3	24	18	55.2	6			43	~20
				08	02	38.20	0.4	24	18	15.8	9			89	~28
194	AB	2	1	08	06	38.34	0.2	42	36	57.4	3	—	155	17	<8
202*	AB	2	1	08	31	58.51	0.1	17	11	07.0	7	—	34	16	<16
204	B	4	2	08	33	16.33	0.4	65	24	05.3	3	32	93	<8	<7
				08	33	21.33	0.4	65	24	04.5	3			<8	<7
205	AB	4	12	08	35	10.19	0.2	58	04	47.6	2	—	12	~17	<8
212	B	4	2	08	55	55.80	0.2	14	21	23.6	12	55	143	<15	<18
				08	55	58.05	0.3	14	20	39.0	16			—	—
215	AB	4	2	09	03	44.34	0.2	16	58	21.3	10	—	134	37	<18
217	AB	2	1	09	05	41.43	0.2	38	00	32.2	3	—	116	15	<11
223	BC	8	2	09	36	48.08	0.2	36	09	47.5	3	292	164	27	10
				09	36	53.62	0.2	36	05	46.4	3			29	16
226	AB	4	12	09	41	36.64	0.3	09	59	58.0	18	34	148	—	<22
228	AB	2	2	09	47	27.85	0.1	14	33	55.0	8	—	9	44	<9
247	AB	2	1	10	56	08.09	0.4	43	17	27.4	3	—	69	13	<10
249.1	ABb	4	2	11	00	24.67	0.5	77	15	08.6	2	—	97	25	~8
254	AB	2	2	11	11	53.31	0.1	40	53	42.0	2	—	110	14	<10
265	B	4	2	11	42	49.73	0.2	31	50	32.6	3	67	107	14	<14
				11	42	54.67	0.2	31	50	15.6	3			<10	<13
277.2	BC	4	2	12	51	03.08	0.1	15	58	36.8	10	43	63	<12	<20
				12	51	05.75	0.2	15	58	57.7	15			—	—
277.3	AB	2	2	12	51	46.12	0.2	27	53	45.0	3	29	154	—	16

TABLE II (*continued*)

Source number	T_b (°K)	Flux density $(10^{-26}\,\mathrm{W\,m^{-2}\,Hz^{-1}})$				Spectral index	Optical identification	References
		S_{1407}	$\pm$	S_{408}	$\pm$			
3C 28	>2600	1·31	0·20	7·3	1·0		Galaxy, $m_v = 17\cdot5$ in cluster	(6), (11)
35	260	—		5·0	0·7	—	Galaxy, $m_v = 14\cdot5$, red	(6), (9)
41	>9700	4·0	0·4	7·2	1·0		(Galaxy, blue, $m_v \sim 20$)	
42	>6700	3·2	0·4	7·9	1·5		Galaxy, $m_v \sim 20$	(9)
44	2000	1·4	0·2	5·2	1·2		(Galaxy, blue, $m_v \sim 20$)	(21)
65	>10000	3·0	0·3	7·9	0·8		—	
68·1	>17000	2·50	0·25	7·2	1·0		—	
	>1400	0·28	0·05					
98	1200	4·9	0·7	24·0	3·0		Galaxy, $m_v \sim 14$	(5), (10), (11), (12)
	2300	5·6	0·8					
111	>21000	5·16	0·5	33·0	3·0		—	(9)
	13000	3·24	0·4					
	>18000	6·0	0·6					
123	120000	51	5	110	18		Galaxy, $m_v \sim 19\cdot5$	(7), (9)
132	>10000	3·57	0·36	7·9	1·0		Galaxy, red, in cluster: $m_v \sim 18\cdot5$	(6), (9)
133	>18000	5·8	0·6	12·6	1·3		—	(9)
169·1	4500	0·58	0·1	3·75	0·5		—	(9)
	>8100	0·82	0·1					
172	>7100	1·18	0·2	7·9	1·6		—	(9)
	8800	1·78	0·2					
175	>960	1·03	0·1	8·5	1·0		QSS, $V = 16\cdot60$	(6), (9), (26)
	>1400	1·53	0·1					
192	>3300	1·69	0·2	10·4	1·5		Galaxy, red, in cluster, $V \simeq 15\cdot4$	(6), (7), (9)
	830	1·13	0·15					
	530	2·08	0·25					
194	>9300	2·0	0·2	5·8	1·0		Galaxy, red, $m_v \sim 20$	
202	>4300	1·75	0·25	3·9	0·6		—	
204	>7600	0·68	0·08	4·6	0·7		QSS, $V = 18\cdot21$	(6), (12), (31), (39)
	>6200	0·55	0·07					
205	>11000	2·38	0·3	7·1	1·0		QSS, $V = 17\cdot62$	(6), (9)
212	>5200	2·21	0·5	8·2	2·0		Galaxy, Type N, $m_v \sim 19\cdot0$	(6), (9), (28)
	580	0·25	0·05					
215	>1500	1·55	0·16	5·6	0·7		QSS, $V = 18\cdot27$	(12), (29), (39)
217	>7400	1·93	0·2	6·3	1·0		—	(9)
223	4700	2·0	0·2	5·3	0·8	0·79	Galaxy, in cluster, $V = 17\cdot1$	(6), (7), (9), (27)
	2000	1·5	0·2	4·2	0·7	0·84		
226	>1900	2·28	0·3	6·7	1·0		Galaxy, red, $m_v \sim 19\cdot5$	(9), (13)
228	>5700	3·6	0·36	9·6	1·5		Galaxy, blue, $m_v \sim 20$	(9)
247	>14000	2·79	0·1	6·92	0·7		—	(20)
249·1	7200	2·3	0·3	6·55	0·7		QSS, $V = 15\cdot72$	(7), (12), (31)
254	>13000	2·96	0·3	10·8	1·0		QSS, $V = 17\cdot98$	(5), (12), (32), (33)
265	>3100	0·96	0·1	11·5	1·4		Double galaxy, $m_v \sim 20$	(6), (9)
	>8300	1·72	0·2					
277·2	>3600	1·36	0·2	6·0	1·0		Galaxy, red, $m_v \sim 19\cdot5$	(9)
	2100	0·68	0·1					
277·3	3200	2·35	0·3	6·75	0·7		Galaxy, $m_v \sim 15\cdot5$ (Coma A)	(5), (9), (11)

TABLE II (*continued*)

Position (1950.0)

Source number	Type	N	Poln	R.A. h	m	s	±s	Dec. °	′	″	±″	θ (″)	p.a. (°)	$\omega_\parallel$ (″)	$\omega_\perp$ (″)
3C 280	AB	2	2	12	54	41·07	0·2	47	36	31·0	3	—	82	14	<9
293	C	4	1	13	49	58·21	0·3	31	42	20·6	4	79	125	—	—
				13	50	01·11	0·3	31	41	53·8	4			—	—
				13	50	03·27	0·1	31	41	33·8	2			<11	<13
294	AB	2	2	14	04	34·12	0·1	34	25	39·5	2	—	31	10	<9
303	AB	4	2	14	41	23·12	0·2	52	14	20·0	3	—	125	12	~8
310	C	8	2	15	02	42·27	0·3	26	14	05·5	4				
				15	02	45·05	0·4	26	13	13·4	5				
				15	02	45·88	0·4	26	14	11·6	5				
				15	02	46·86	0·3	26	12	20·9	4	250	~150	—	125
				15	02	48·83	0·4	26	11	15·4	4				
				15	02	50·80	2·0	26	13	20	30				
314·1	C	8	12	15	09	57·04	0·7	70	58	13·8	3	180	—		
				15	10	00·25	0·7	70	57	55·3	3			48	~30
				15	10	11·56	0·5	70	57	06·4	3				
				15	10	11·88	0·5	70	56	34·0	3			70	40
				15	10	23·17	0·7	70	56	47·8	3			—	—
315	C	8	2	15	11	28·31	0·3	26	19	01·3	3	—	—	—	—
				15	11	30·73	0·3	26	18	23·0	3			—	—
320	A	2	2	15	29	29·72	0·2	35	43	49·5	2	—	77	17	<12
321	AB	2	2	15	29	40·83	0·2	24	12	47·9	2	—	100	14	<17
325	AB	2	2	15	49	14·30	0·2	62	50	19·8	2	—	118	17	<8
326	C	16	12	15	49	06·4	1·0	20	12	00	25	1060	80	~120	<100
(at				15	49	33·4	1·0	20	13	07	25			166	~146
408 MHz)				15	49	45·2	1·0	20	12	48	25			—	<100
				15	50	12·6	1·0	20	14	45	25			153	<100
336	AB	2	2	16	22	32·43	0·1	23	52	10·6	5	—	29	28	<12
351	BC	4	12	17	04	01·10	0·5	60	47	59·8	4	59	34	~19	~10
				17	04	05·54	0·2	60	48	49·2	2			<11	<8
365*	AB	4	1	17	56	13·23	0·1	13	28	50·4	9	—	2	<30	<7
386	C	8	2	18	36	12·18	0·3	17	08	07·2	14	—	~26	~220	~110
				18	36	13·58	0·3	17	09	22·8	14				
388	B(b)	4	2	18	42	34·21	0·2	45	30	19·4	3	26	66	~16	~16
				18	42	36·49	0·2	45	30	29·7	3			<12	<12
401	AB	2	2	19	39	38·87	0·1	60	34	30·5	2	—	25	16	<8
409	AB	4	1	20	12	18·23	0·2	23	25	47·5	8	—	146	26	<13
432	AB	2	2	21	20	25·49	0·1	16	51	49·0	7	—	126	12	<20
433	AB	4	1	21	21	30·52	0·1	24	51	17·4	2	~52	31	—	~11
435	BC	4	2	21	26	36·86	0·2	07	19	46·0	15	32	83	<10	<80
				21	26	38·98	0·2	07	19	48·8	15			<20	~150
435·1	C	4	1	21	33	47·6	3	83	44	18·6	3	3348	~0	<25	<25
				21	34	13·5	3	84	40	06·5	3			<25	<25
				21	35	51·9	2	84	16	46·4	2			<15	<15
437	AB	4	12	21	45	01·30	0·2	15	06	53·5	12	—	162	43	<12
438	AB	4	1	21	53	45·66	0·1	37	46	14·4	2	—	129	27	<10
441	AB	2	2	22	03	48·72	0·2	29	14	51·5	4	29	150	—	<10
442	C	8	2	22	12	11·7	1·4	13	35	22·6	10	270	69	155	<85
(at				22	12	28·9	1·4	13	36	08·0	10			200	<85
408 MHz)				22	12	42·2	1·0	13	07	35·7	10			—	<35
449	C	8	12	22	29	06·19	0·3	39	08	28·5	4	~300	—	—	—
				22	29	06·19	0·2	39	07	25·4	2			~13	~12
				22	29	06·40	0·2	39	04	18·2	2			30	~13
				22	29	07·26	0·2	39	05	43·2	4			—	<10
				22	29	08·02	0·2	39	06	37·8	4			—	<10
470	ABb	2	2	23	56	02·47	0·2	43	47	56·9	2	—	37	<12	<9

TABLE II (*continued*)

Source number	T_b (°K)	S_{1407}	±	S_{408}	±	Spectral index	Optical identification	References
3C 280	>24000	4·86	0·5	12·2	1·5		—	
293	1500	0·33	0·1					
	1000	0·23	0·1	10·7	2·0		Galaxy, $m_v \sim 14·3$	(6), (9), (13), (27)
	>19000	4·24	0·4				+ companions	
294	>9800	1·4	0·14	5·7	1·0		—	(20)
303	16000	2·5	0·3	6·3	0·8		(Cluster of galaxies)	(6), (9), (13)
310								
	280	7·6	1·0	30·2	3·0		Triplet of galaxies, $m_v \sim 14·5$	(5), (10), (11)
314·1								
	110	0·26	0·1					
				9·2	2·0		Galaxies, in cluster	(6), (9)
	260	1·14	0·2					
315	930	3·7	0·4	9·8	2·0		Two galaxies, $m_v \sim 16·6$ + 16·2	(5), (10), (11)
320	>5400	1·75	0·2	5·5	0·8		Galaxy, red, in cluster, $m_v \sim 18$	(6), (9)
321	>7100	2·67	0·3	7·1	1·0		—	
325	>19000	4·1	0·5	10·0	1·5		—	
326	>10			1·25	0·2			
	10	3·4	0·6	2·97	0·4		Part of North Galactic Spur	(6), (9)
	>38							
	>91			5·42	0·8			
336	>5600	3·0	0·5	6·9	1·0		QSS. $V = 17·47$	(12), (29)
351	1200	0·36	0·15	6·8	1·5		QSS, $V = 15·28$	(6), (9), (23)
	>21000	2·94	0·25					
365	>8900	2·98	0·3	6·9	1·0		—	(8)
386	180	7·0	0·7	14·8	2·0		Supernova Remnant	(5), (10), (11), (40)
388	6800	2·77	0·3	13·5	2·0		Double galaxy; $m_v = 14·5$ with companion	(5), (10), (11)
	>14000	3·23	0·3					
401	>26000	5·2	0·5	11·0	1·5		Galaxy, red, $m_v \sim 19$	(6), (7), (8)
409	>26000	—		—			—	(9)
432	>3900	1·49	0·15	5·1	0·7		QSS, $V = 17·96$	(6), (9), (31)
433	12000	11·0	1·5	28·0	4·0		Double glaxy, $m_v \sim 16·0$	(5), (8), (10), (11)
435	>1200	1·5	0·2	6·5	1·0		—	(20)
	>130	0·6	0·1					
435·1	>1100	1·07	0·2	3·5	0·5	0·91	—	
	>310	0·31	0·1	2·6	0·5	1·72	—	
	>1300	0·46	0·1	0·7	0·2	0·34	(20^m blue object)	
437	>4000	3·3	0·5	8·8	1·2		—	
438	>15000	6·3	1·0	29	7·0		—	
441	>6100	2·8	0·3	7·3	1·0		—	
442	>67	3·0	0·4	9·9	1·5	0·97	Double galaxy, 13^m·8 + 14^m·5 plus companion	(5), (6), (10)
	>56							
	>120	0·97	0·2	2·44	0·5	0·74		
449	420	0·12	0·02					
	2300	0·56	0·10					
	2100	1·30	0·20	6·5	1·0		Galaxy, in cluster, $m_v = 12·5$	(6), (9), (41)
	>1000	0·33	0·05					
	>600	0·19	0·03					
470	>13000	2·24	0·25	5·3	0·7		Galaxy, red, $m_v \sim 19·5$	(9)
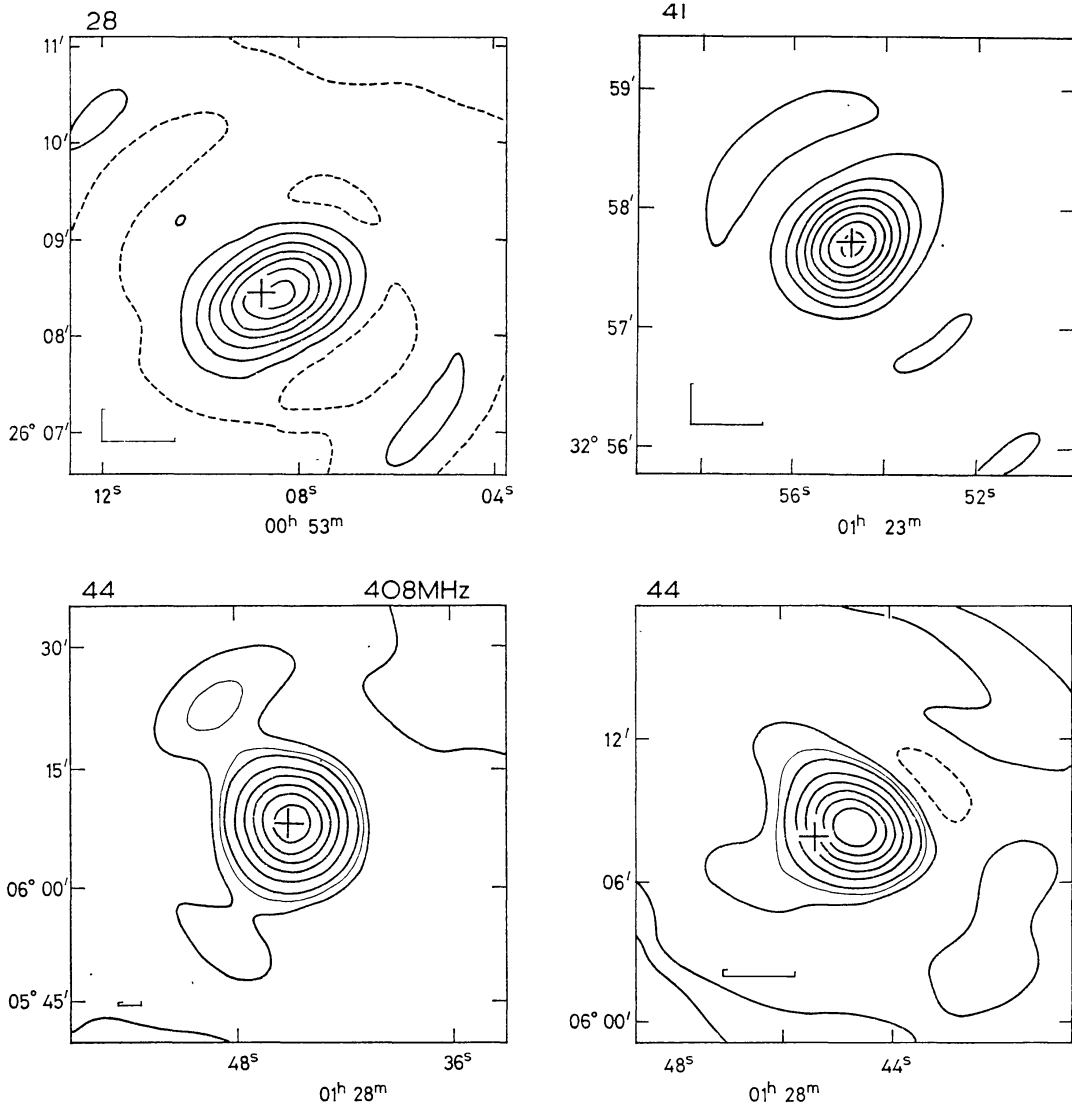
FIG. 1. *3C 28. The cross marks a $17^m \cdot 5$ red galaxy, in a cluster. The redshift is $0 \cdot 1959$ (S, V).*

3C 41. The object marked by a cross is a very faint $\sim 20^m$ diffuse object, visible only on the blue print, near the limiting magnitude. The object may be a print defect.

3C 44. The structure of this source is different at each frequency and maps at both 408 MHz and 1407 MHz are given. The present observations show large scale sctructure not found by Taylor & de Jong (21) from lunar occultation studies. The object marked is a faint blue diffuse object, possibly just visible on the red print.
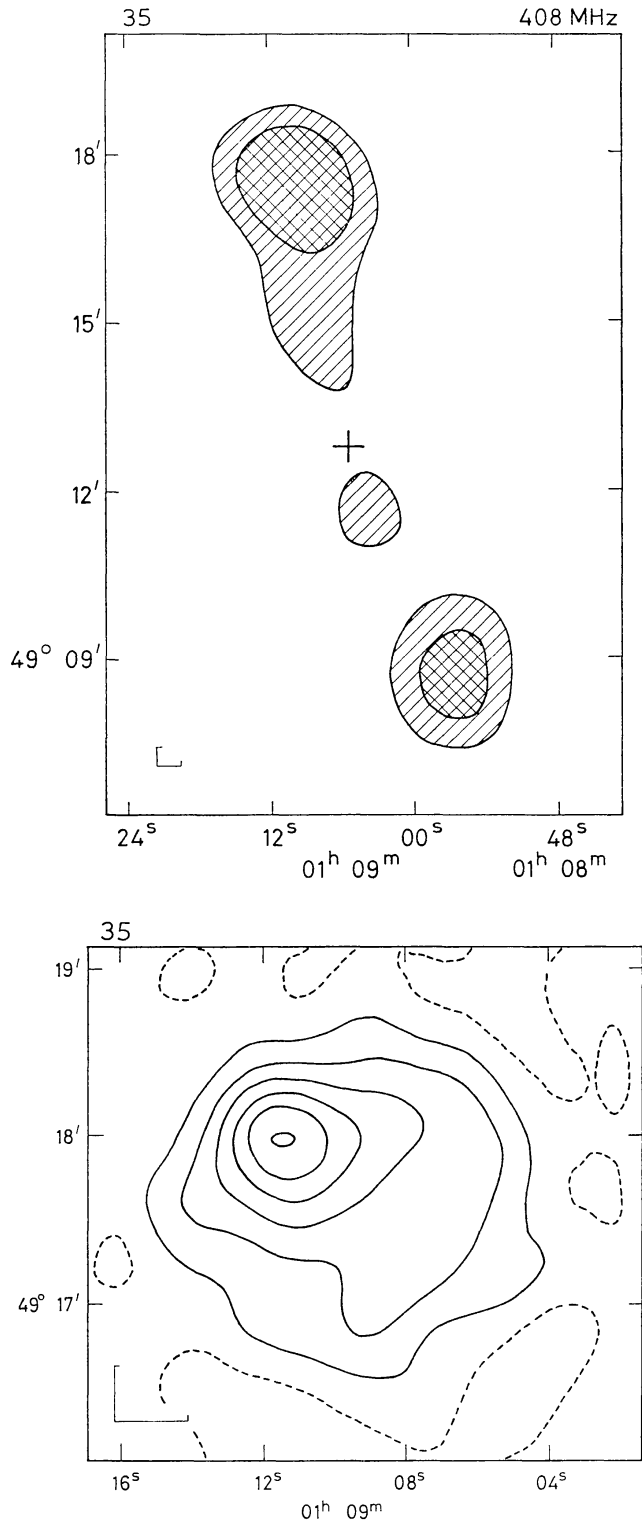
Fig. 2. *3C 35. Maps at both frequencies are given. At 408 MHz, the extreme components lie in the grating responses of the other component, and only a sketch map is given, from which the grating rings have been removed. The cross marks the position (V) of a $14^m \cdot 5$ red galaxy in a group (W2). At 1407 MHz, only one component is observed, of large extent and low brightness (see Notes).*
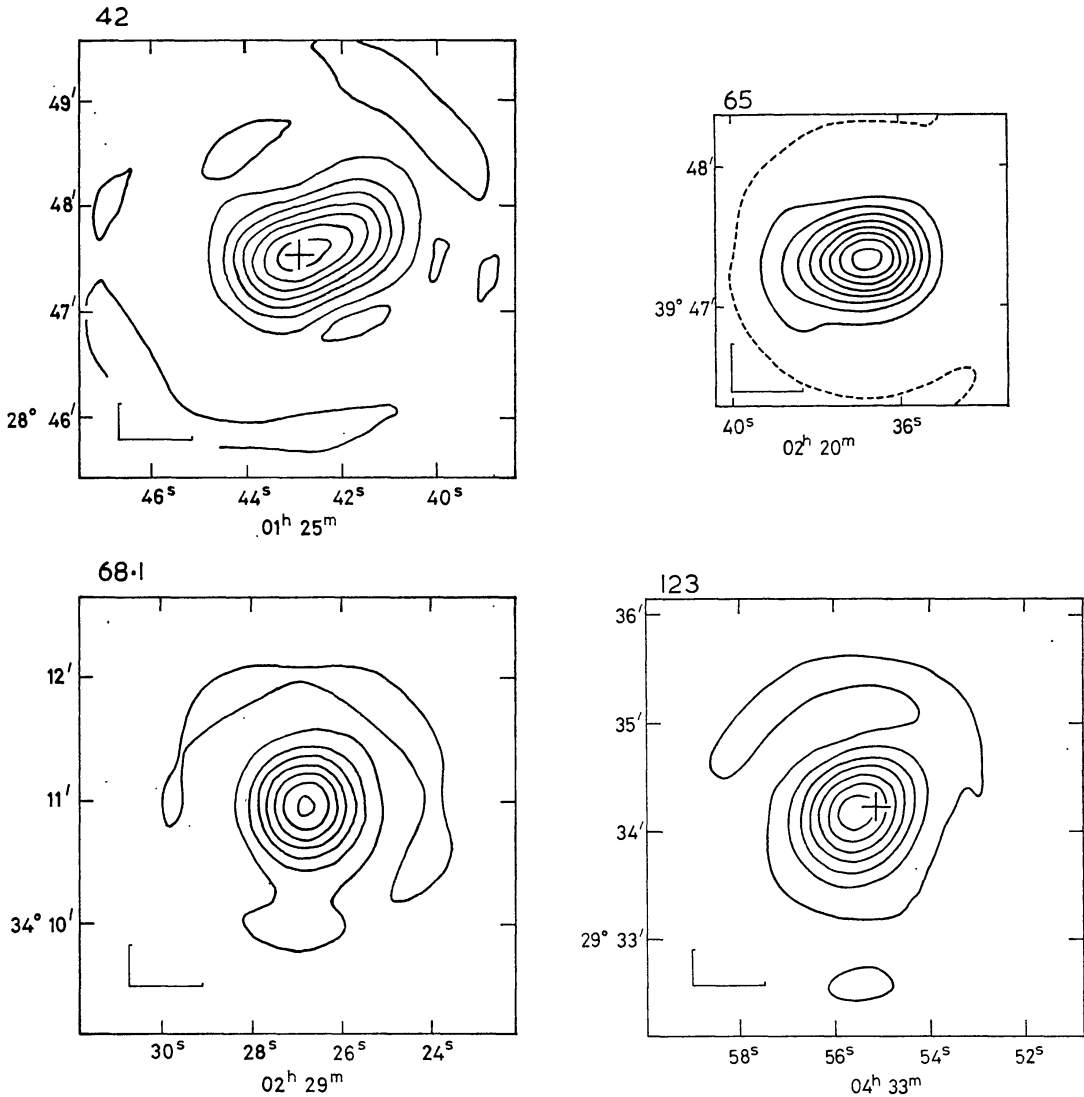
FIG. 3. *3C 42. The observations are well fitted by a simple double model, with unresolved components 26″ arc apart having a flux density ratio of 1·34:1 at 1407 MHz. The cross marks a very faint ∼20ᵐ galaxy suggested by Wills (private communication); it is of neutral colour and at the limit on both red and blue prints (W2).*

3C 65. The observations are consistent with those made by Adgie & Gent (22). They are well fitted by a simple double model with unresolved components 16″ arc apart having a flux density ratio of 2·5:1 at 1407 MHz. There is an 18ᵐ·6 object of neutral colour some 12″ south of the peak; it is probably a star (W2). The field is otherwise blank.

3C 68·1. There is no object within 30″ of this source (W2).

3C 123. The cross marks a 19ᵐ·5 galaxy (L, W2).
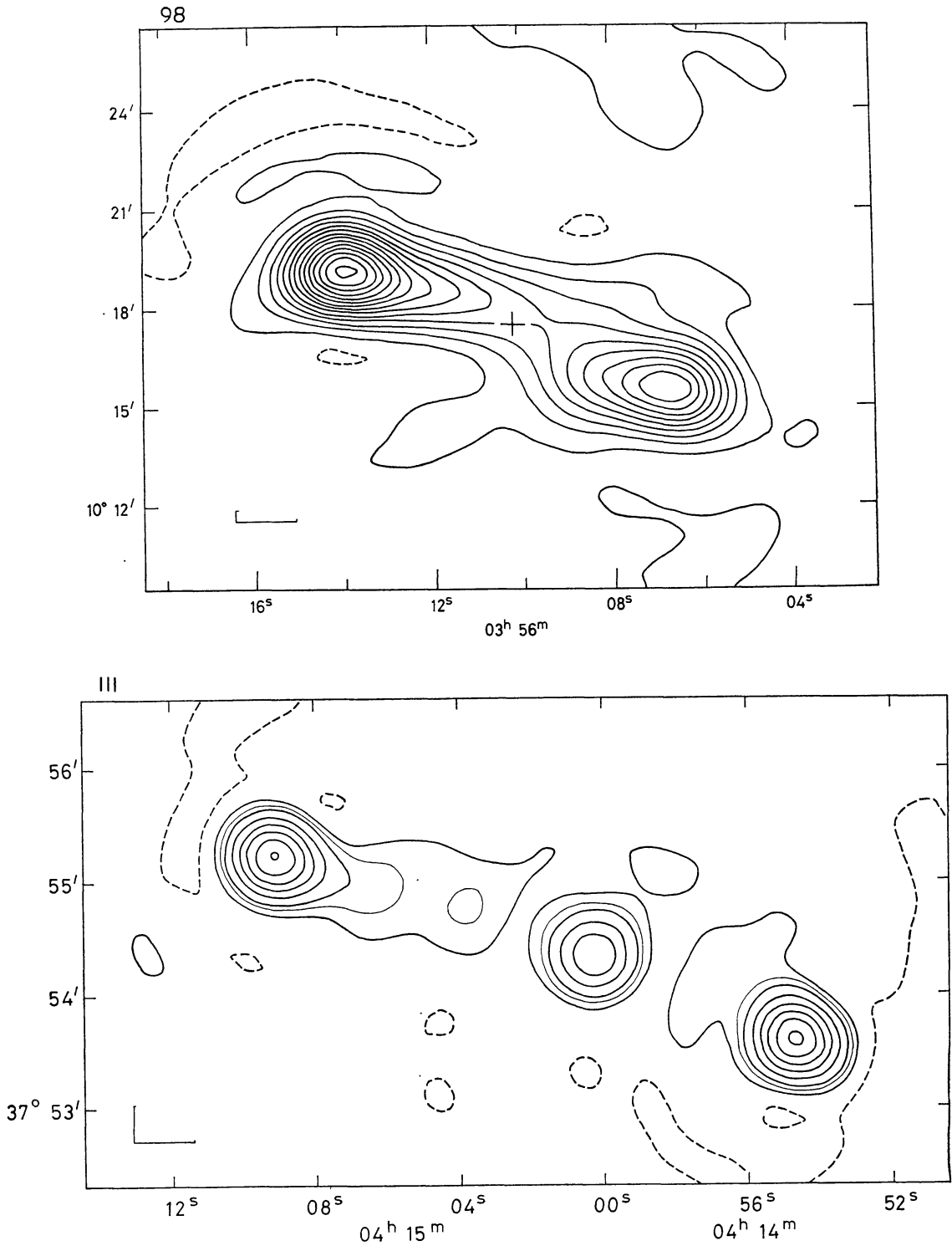
Fig. 4. *3C* 98. *Although the 408 MHz observations do not resolve the source into two components, convolution of the 1407 MHz map with the 408 MHz beam shows that the spectrum of the west component is steeper than that of the east component. The cross marks a* 14^m *galaxy. There are a number of other objects in the field of this source, mostly stellar in appearance* (**23**) (*MMS, S*). *The redshift of the galaxy in* 0·0306.

     3C 111. *A comparison with the 408 MHz observations shows that the two outermost components have appreciably steeper spectra than the innermost components. There are a number of red stellar objects in the field of this source, which is heavily obscured* ($b^{II} = -9°$) (*W2*).
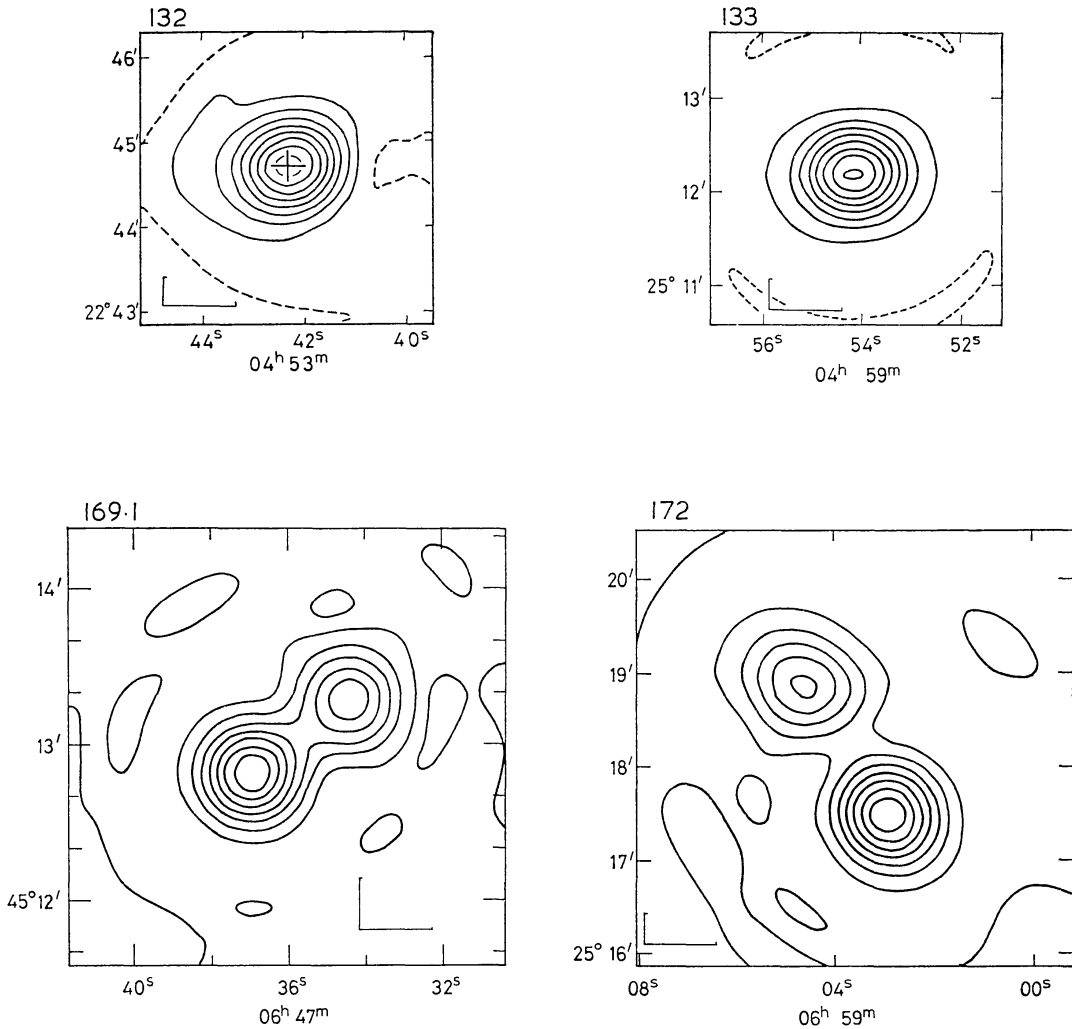
FIG. 5. 3C 132. *The present observations confirm the conclusions reached by de Jong* (**24**) *and disagree with those of Taylor* (**25**) *from lunar occultation studies of this source. The cross marks a red* $18^m\cdot5$ *galaxy in a cluster, some* 5″ *West of a* $16^m\cdot7$ *stellar object* (V, W2).

3C 133. *The observations are consistent with that found by Taylor & de Jong* (**21**) *from lunar occultation studies of the source. The field of this source is heavily obscured* (W2).

3C 169·1. *There may be some very faint objects in the field of this source, but it is otherwise blank* (W2).

3C 172. *There are a number of faint objects in the field of this source.*
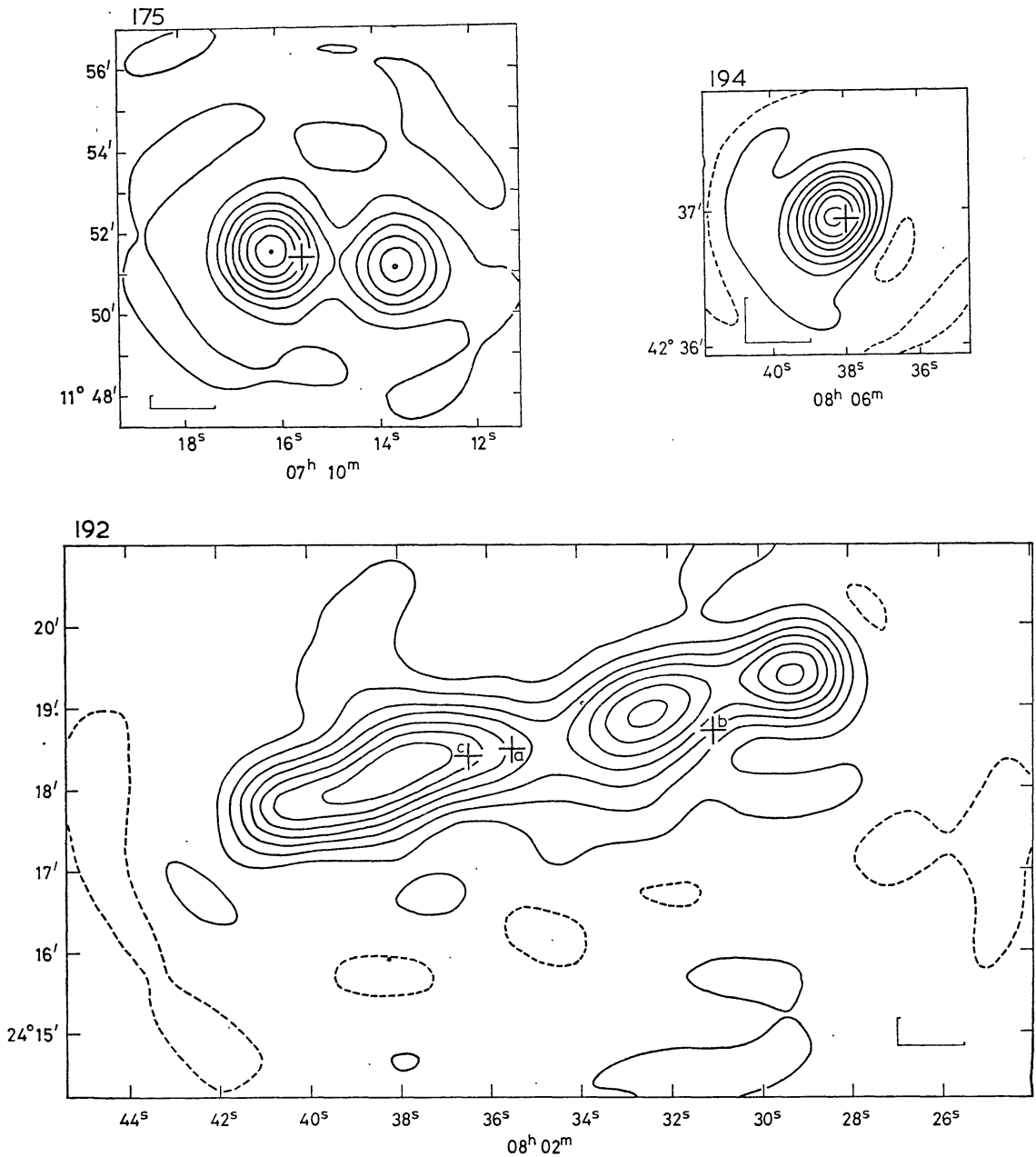
FIG. 6. *3C 175. The cross marks the position of a* $V = 16^m \cdot 60$ *quasi-stellar source (QSS) with redshift* $0 \cdot 768$ *(W, V)* (26).

3C 194. The cross marks a $20^m \cdot 0$ *possibly diffuse red object, probably a galaxy, which has been measured by Parker (private communication) and is close to the radio position.*

3C 192. The well resolved eastern component has a steeper spectrum than the two more compact sources to the west of the source. The structure found at 1407 MHz is similar to that found at 256 MHz by Taylor & de Jong from lunar occultation studies (21). *Their observations confirm that the most easterly component has a steeper spectrum, and the most westerly component a flatter spectrum. The objects marked are (a) red* $V = 15^m \cdot 4$ *galaxy in a cluster, redshift* $0 \cdot 0596$. *(b) Another red galaxy,* $15^m \cdot 0$. *(c) A stellar object,* $14^m \cdot 4$ *of neutral colour (L, V, W2)* (27).
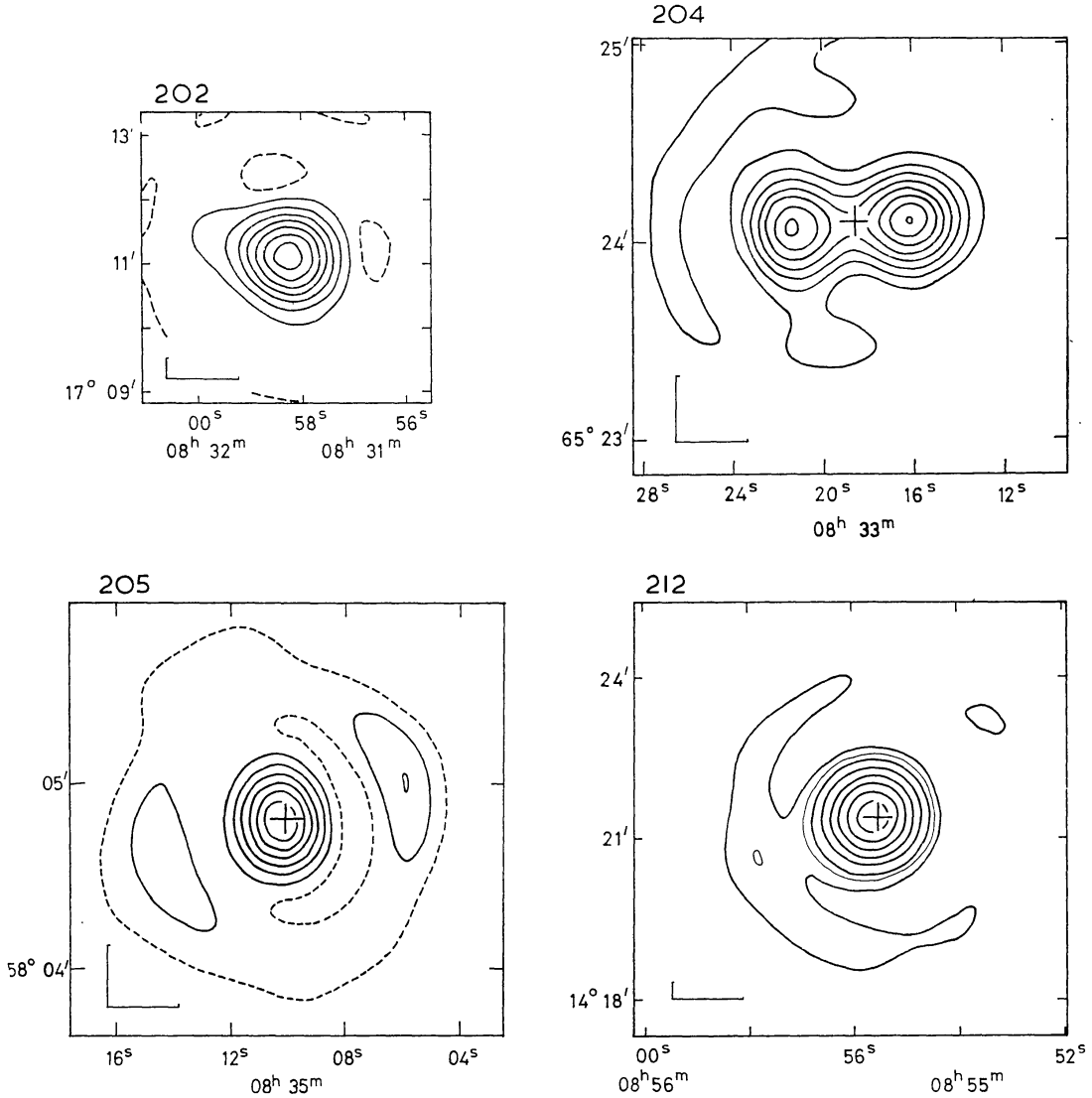
FIG. 7. *3C 202. The field is blank at the radio position. There are no objects within 30″ of either radio peak (see Notes).*

3C 204. The cross marks a $V = 18^{m} \cdot 21$ QSS with a redshift of $1 \cdot 112$ (SVW).
3C 205. The cross marks a $V = 17^{m} \cdot 62$ QSS, redshift $1 \cdot 534$ (W2, V).
*3C 212. The object marked is a $19^{m} \cdot 0$ N-type galaxy (**28**).*
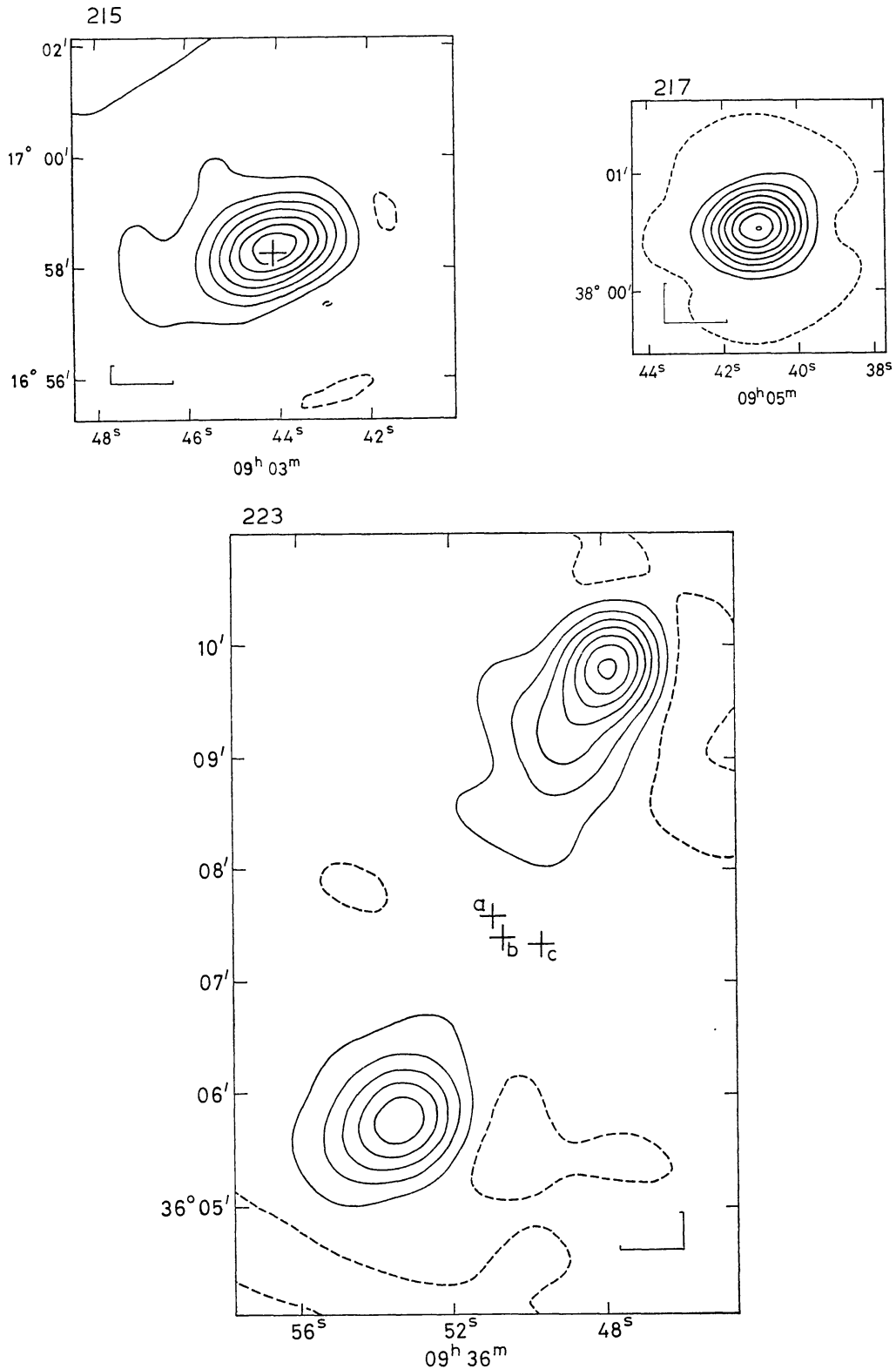
FIG. 8. *3C 215. The cross marks a $V = 18^m \cdot 27$ QSS (SVW) with redshift 0·411 (29). There may be a jet extending to the South-East of the QSS, parallel to the radio axis. There is also a $\sim 17^m$ red stellar object some 11″ to the South-East (W2).*

3C 217. Blank field at the radio position. There are no objects within 30″ arc on the Sky Survey prints (W2).

3C 223. (a) red $V = 17^m \cdot 1$ galaxy in a cluster with a redshift of 0·1367 (27). (b) and (c) are two close cluster members, $18^m \cdot 5$ and 19^m respectively, each being red in colour (L, V). This source shows no appreciable change of structure with frequency.
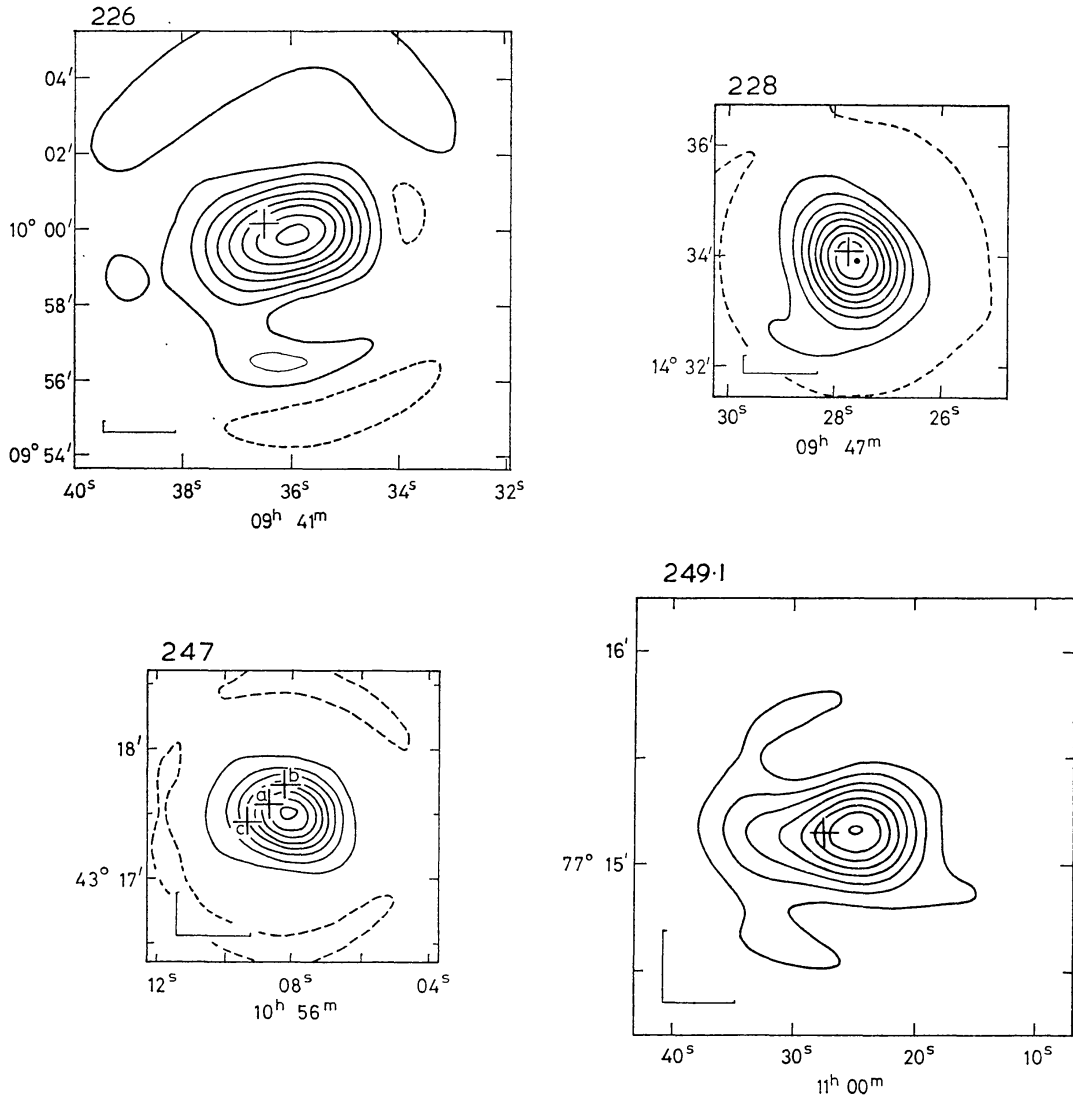
FIG. 9. *3C 226. The cross marks a faint* $19^m \cdot 5$ *red galaxy (WP). There are no other objects within* $30''$ *arc of the radio peak (W2).*

3C 228. The cross marks a 20^m *blue object, probably a galaxy (W2). The observed structure is consistent with the lower limit given by Anderson* et al. *(30) from long baseline interferometry.*

3C 247. (a) $V = 18^m \cdot 82$ *(SVW) sub-dwarf (19), probably not related (20). (b) Blue galaxy,* $19^m \cdot 5$ *(c) Red galaxy,* $19^m \cdot 5$. *There may be another, fainter galaxy nearer the radio peak, but it is visible only on the red print (SVW) (W2).*

3C 249.1. The cross marks the position of a $V = 15^m \cdot 72$ *QSS (L, SVW) with a redshift of* $0 \cdot 3107$ *(31). It is found to be optically variable (Penston & Cannon, private communication).*
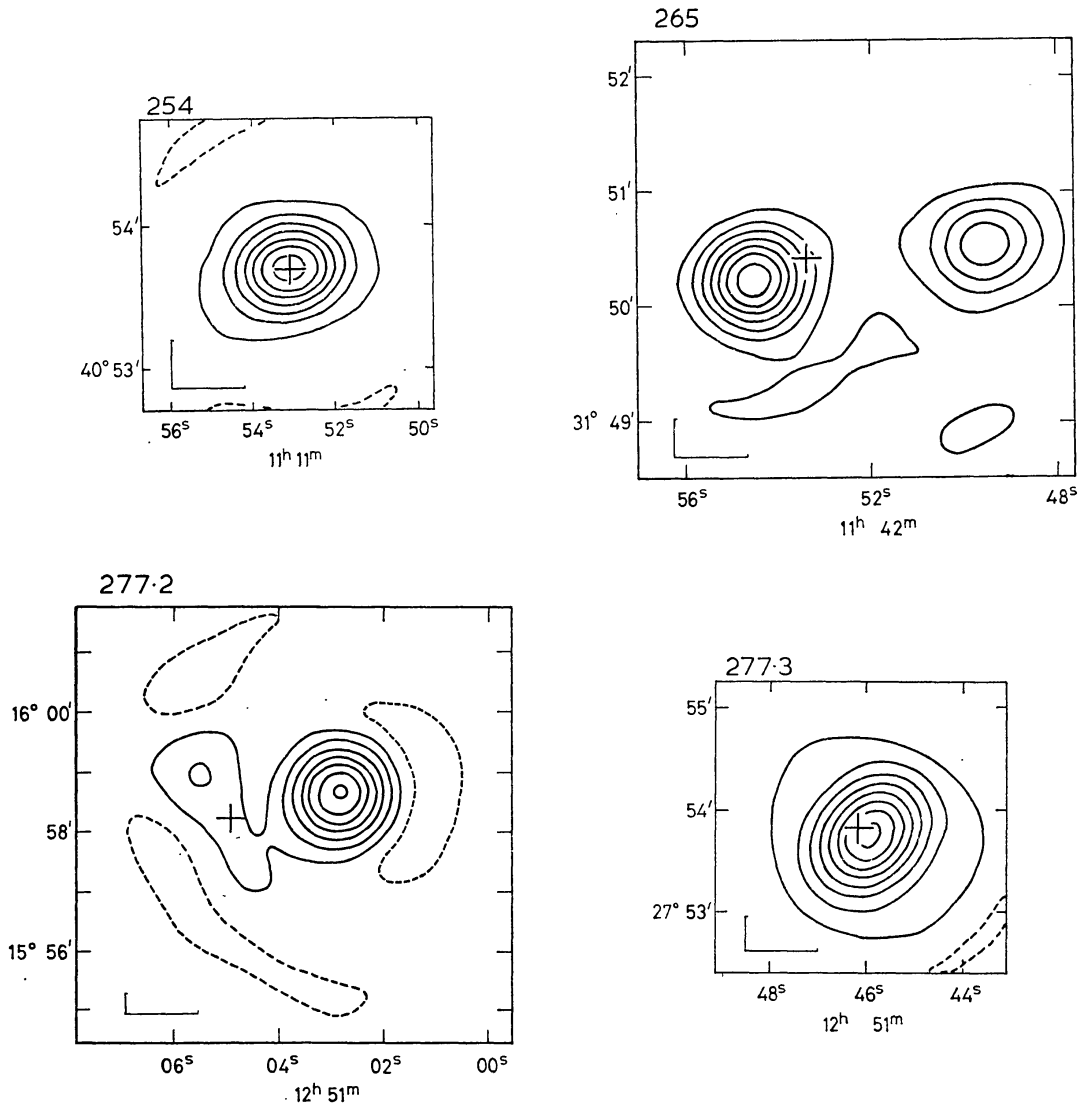
FIG. 10. *3C 254. The cross (G) marks a $V = 17^m \cdot 98$ QSS, redshift $0 \cdot 734$ (32, 33). The present observations are in agreement with those of Clark & Hogg (34).*

3C 265. The cross marks the position of a 20^m pair of objects, probably galaxies (W2). The axis of the radio double is parallel to the axis of the double galaxy. There are no other objects in the field.

3C 277.2. The cross marks the position of a $19^m \cdot 5$ red galaxy (W2). There are no other objects in the field.

3C 277.3 Coma A. The observations are well fitted by a simple double model with components of equal flux density and a Gaussian half-power width of about $16''$ arc, $50''$ arc apart. The cross (G) marks a $15^m \cdot 5$ galaxy, redshift $0 \cdot 0857$ (S). The object is symmetrical and slightly diffuse on the red print. On the blue print, the nucleus is irregularly extended to the South-East. There is a large ($\sim 60''$) diffuse optical envelope parallel to the radio axis.

4
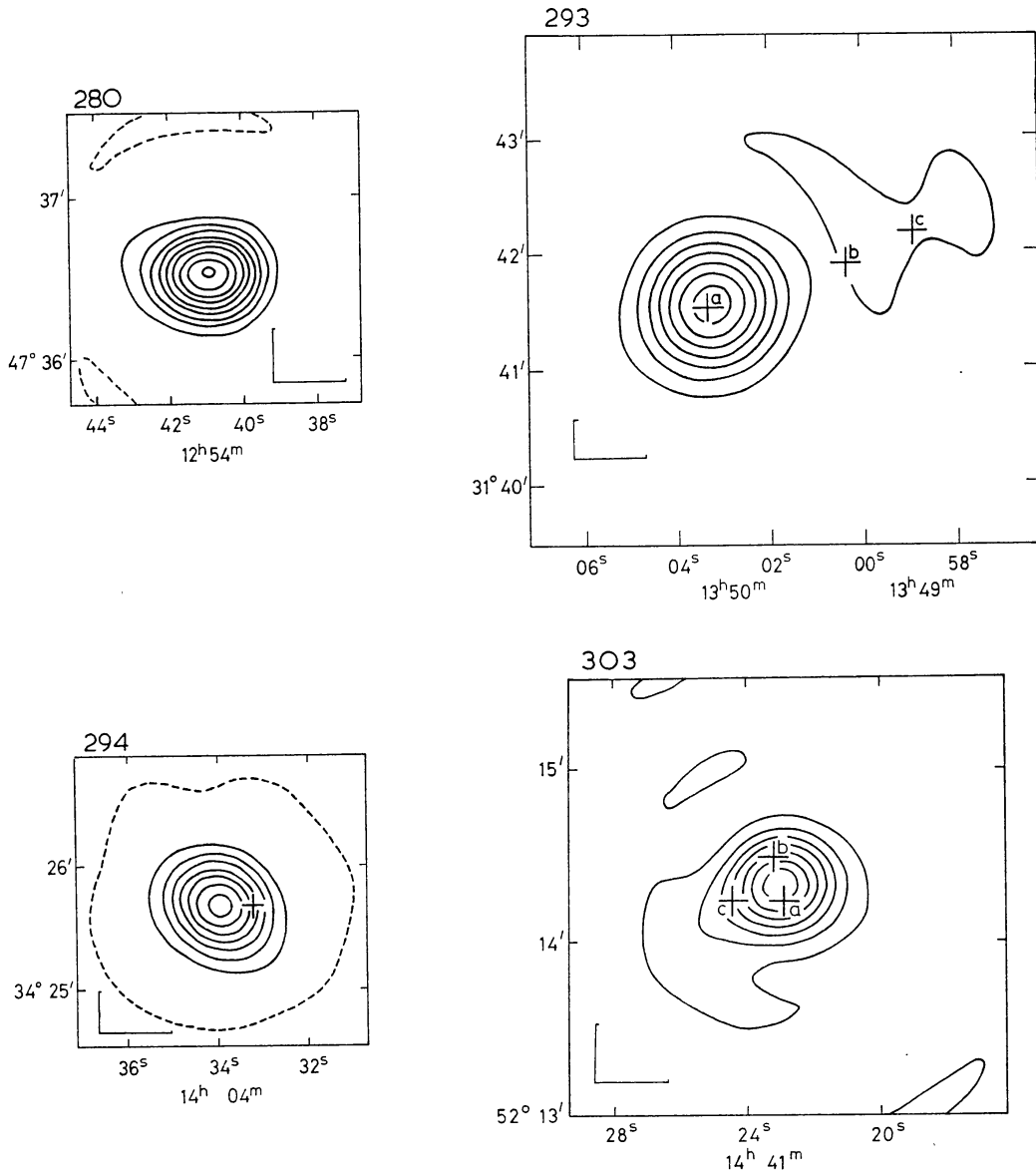
FIG. 11. 3C 280. *The structure found in the present observations is consistent with that found by Clark & Hogg* (**34**). *There are no objects within* 30″ *arc of the radio peak* (W1).

3C 293. *The two faint components have much steeper spectra than the main bright component. The distribution of faint sources in the field of this source is most unusual. The objects marked are* (a) *galaxy*, $14^m \cdot 3$, *redshift* $0 \cdot 0452$ (W2) (**27**), (b) *faint* $19^m \cdot 5$ *red galaxy*, (c) *neutral colour object, close to print limit on both red and blue prints.*

3C 294. *The cross marks an* $11^m \cdot 8$ *F-type star* (W2), *which is probably unrelated to the radio source* (**20**). *There is no other object in the field of the source.*

3C 303. *The radio position is in the middle of three objects.* (a) *is a blue* 19^m *object, stellar on red, diffuse on the blue print.* (b) (*object 'a' of WP*) *is red, diffuse, and appears double on the red print.* (c) *is a red* 16^m *galaxy, the brightest in the cluster* (W2, V).
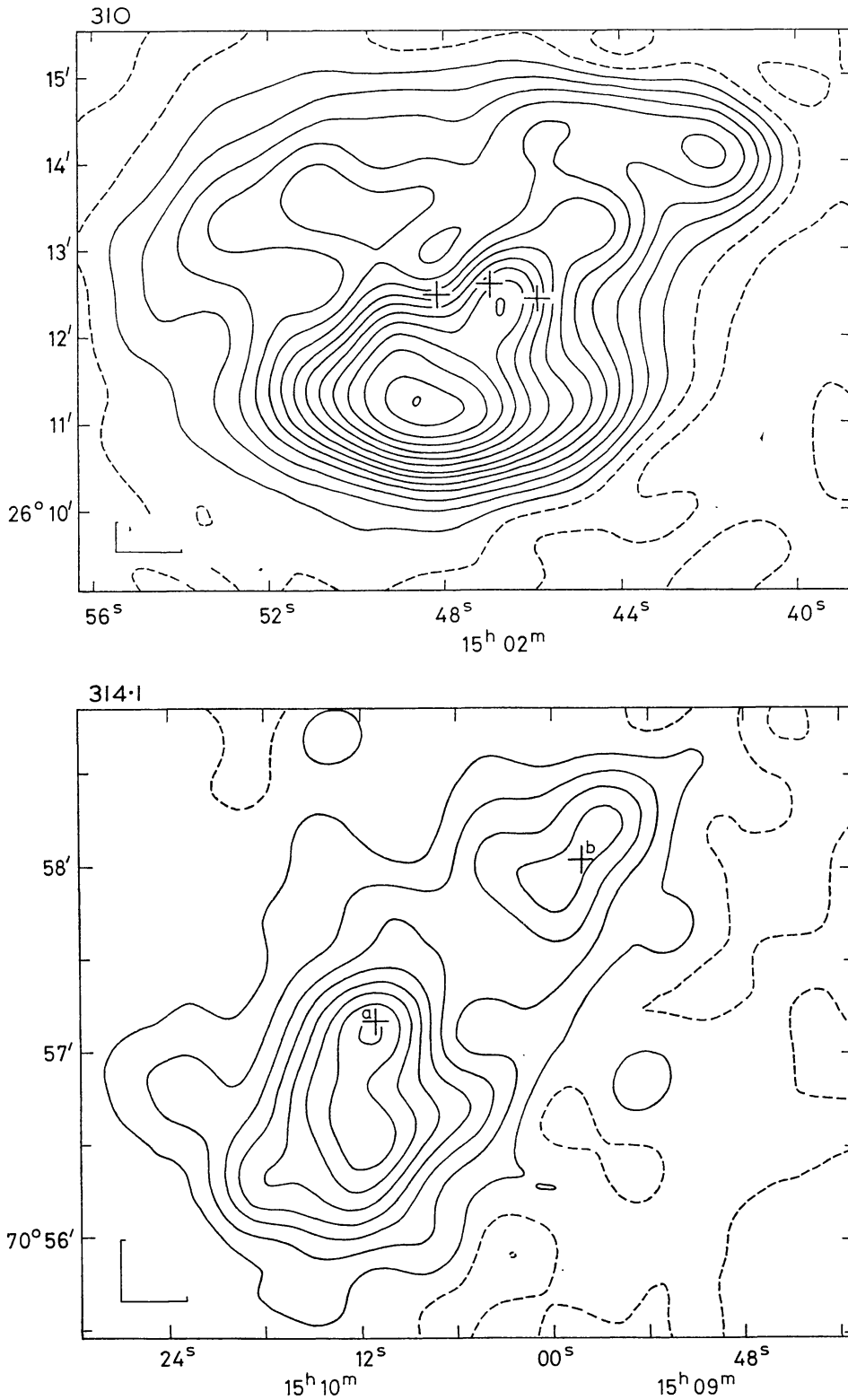
FIG. 12. 3C 310. *The large, low brightness region to the North-East of the source has a flatter spectrum than the rest of the source. The crosses mark a* $14^m \cdot 5$ *triplet of galaxies, VV 4-36-4/5 (35) in a cluster. The redshift is* $0 \cdot 0543$ *(MMS, S).*

3C 314·1. *The North-West component may have a slightly flatter spectrum than the brighter South-East component.* (a) $17^m \cdot 0$ *red galaxy (W2).* (b) $19^m \cdot 0$ *red galaxy. There are a number of other galaxies in the field of this source, probably cluster members with* (a) *and* (b) *(V).*
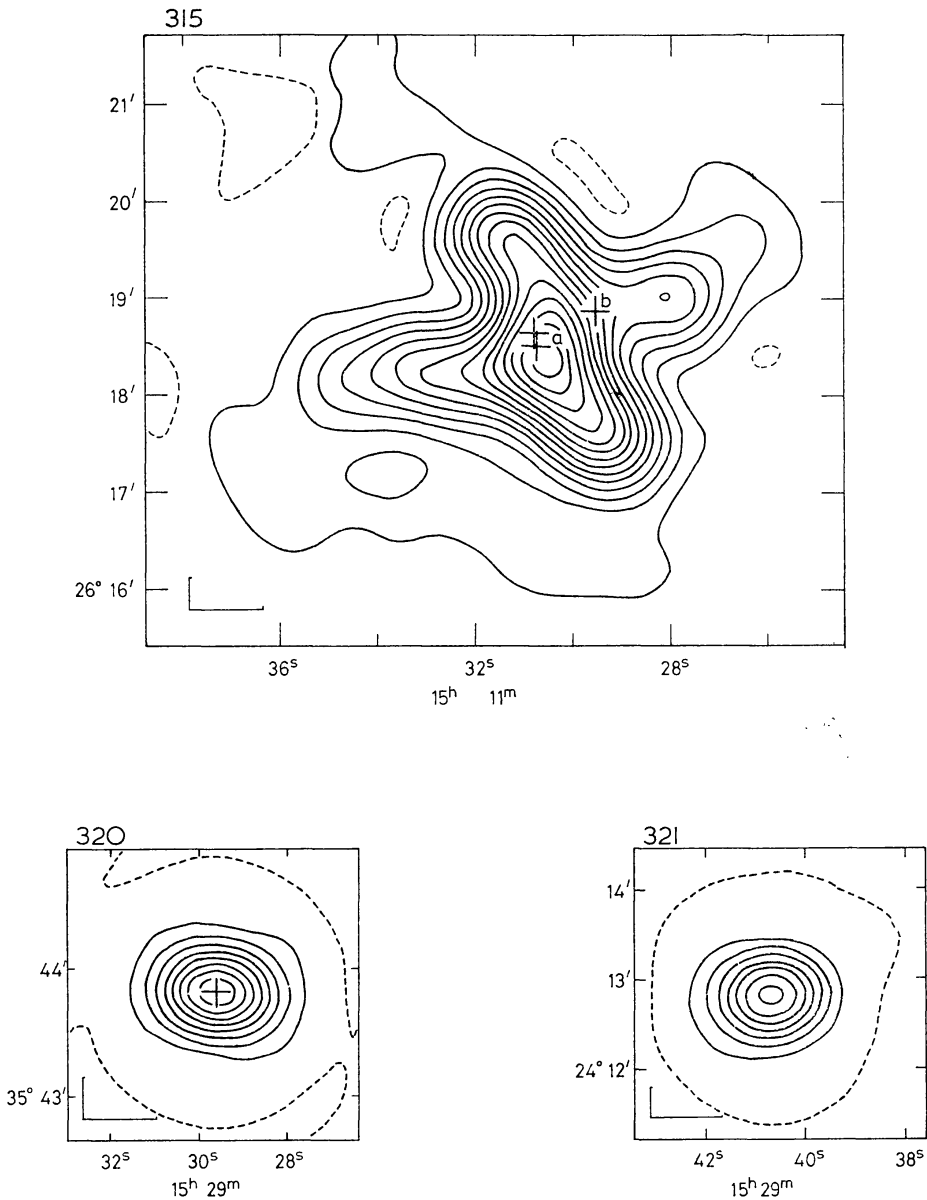
FIG. 13. *3C* 315. *The North-West–South-East arm of this source may have a slightly flatter spectrum than the rest of the source. (a) Pair of galaxies,* $16^m \cdot 6$ *and* $16^m \cdot 2$ *in a common envelope. (b)* $19^m \cdot 5$ *blue galaxy, stellar on red print, diffuse on the blue print. There are many other galaxies in the field of this source (MMS, S, G). A redshift of* $0 \cdot 1086$ **(11)** *is found for the North-East galaxy of the pair.*

3C 320. *The cross marks an* 18^m *red galaxy in a cluster (W2).*

3C 321. *There are no objects within* $25''$ *of the radio position (W1).*
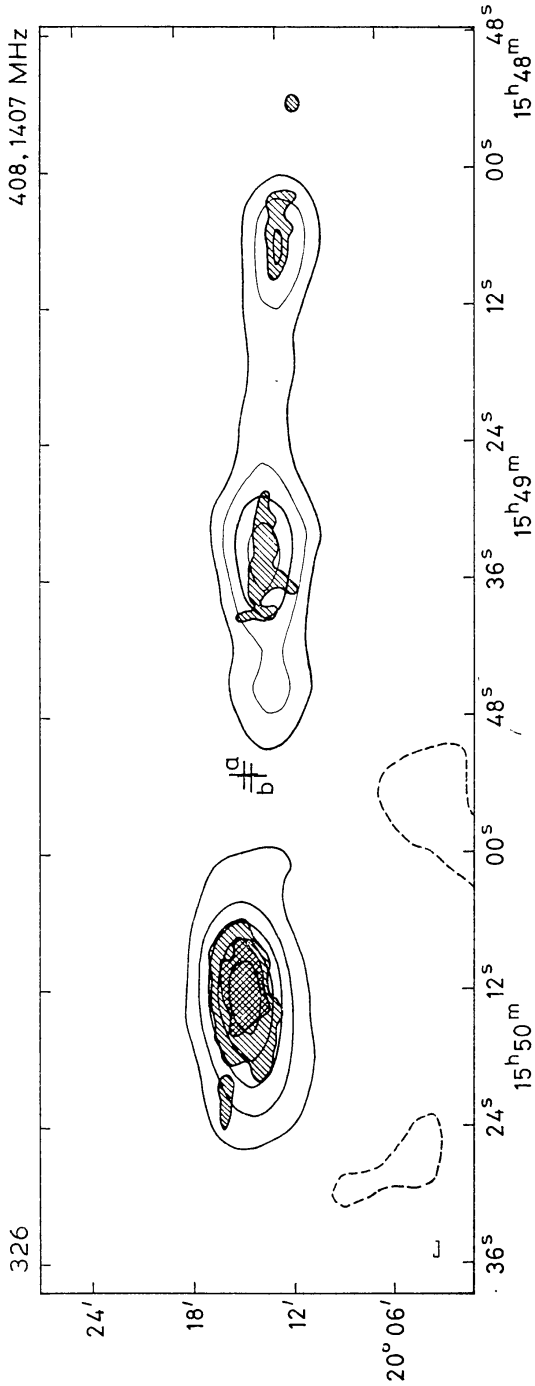
FIG. 14. 3C 326. *The map presented is that made at 408 MHz with the structure found at 1407 MHz cross-hatched in. The objects marked are (a) 17ᵐ red galaxy and (b) 17ᵐ·5 red galaxy in a very large cluster of galaxies (W2). J. E. Baldwin has pointed out (private communication) that 3C 326 is centred on a ridge of the North Galactic spur and runs exactly parallel to it. In view of the particularly low brightness temperatures found, there is a strong possibility that 3C 326 might be a galactic radio source.*
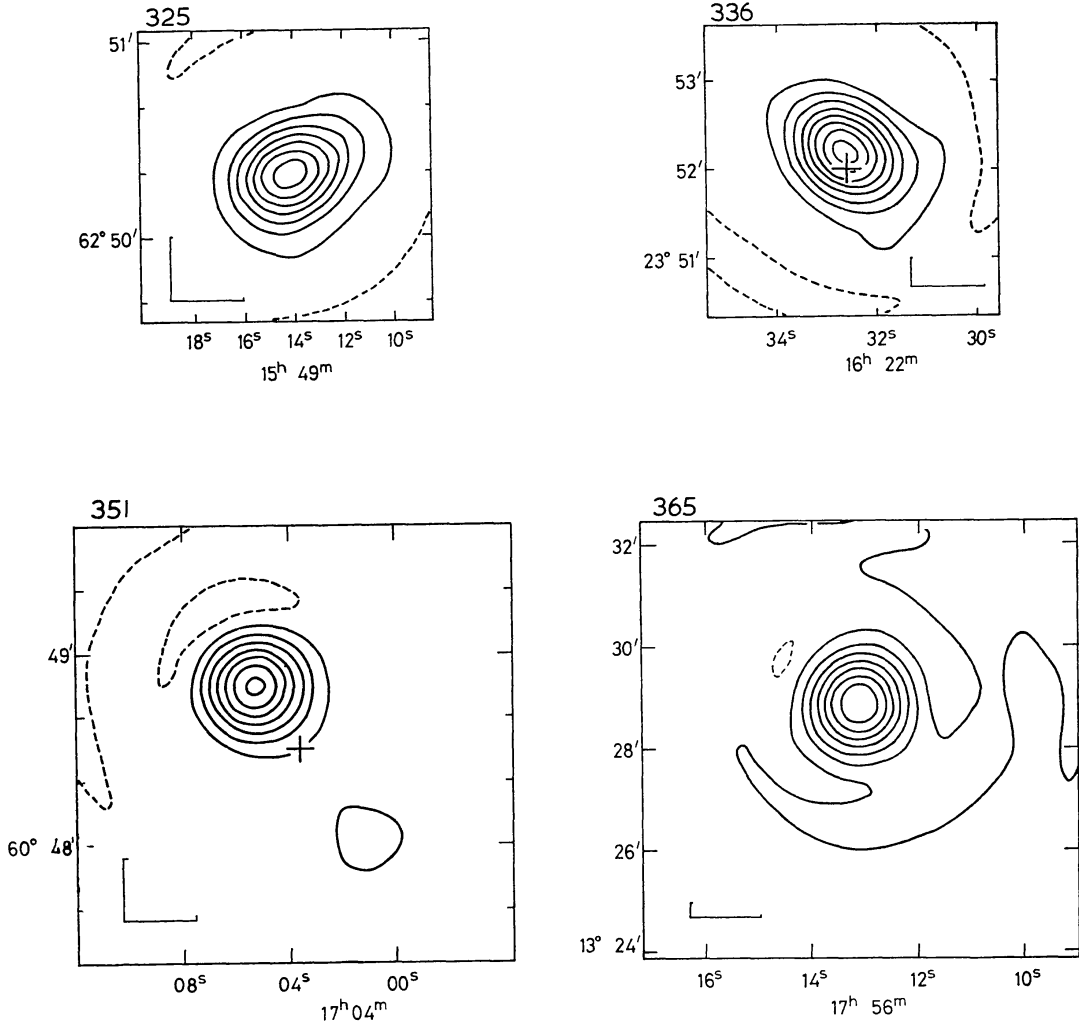
FIG. 15. *3C 325. Nothing visible at the radio position (W2).*

3C 336. The object marked is a $V = 17^m \cdot 47$ *QSS with a redshift of* $0 \cdot 927$ *(SVW)* (**29**).

3C 351. The object marked is a $V = 15^m \cdot 28$ *QSS, with redshift* $0 \cdot 371$ *(W2)* (**23**).

3C 365. There are a number of faint red objects at print limit in the field of this source, which is quite crowded as it is close to the galactic plane (W1). There is a low brightness region of $\sim 150''$ *arc total extent to the South of the main peak, which accounts for some 10 per cent of the flux at 1407 MHz.*
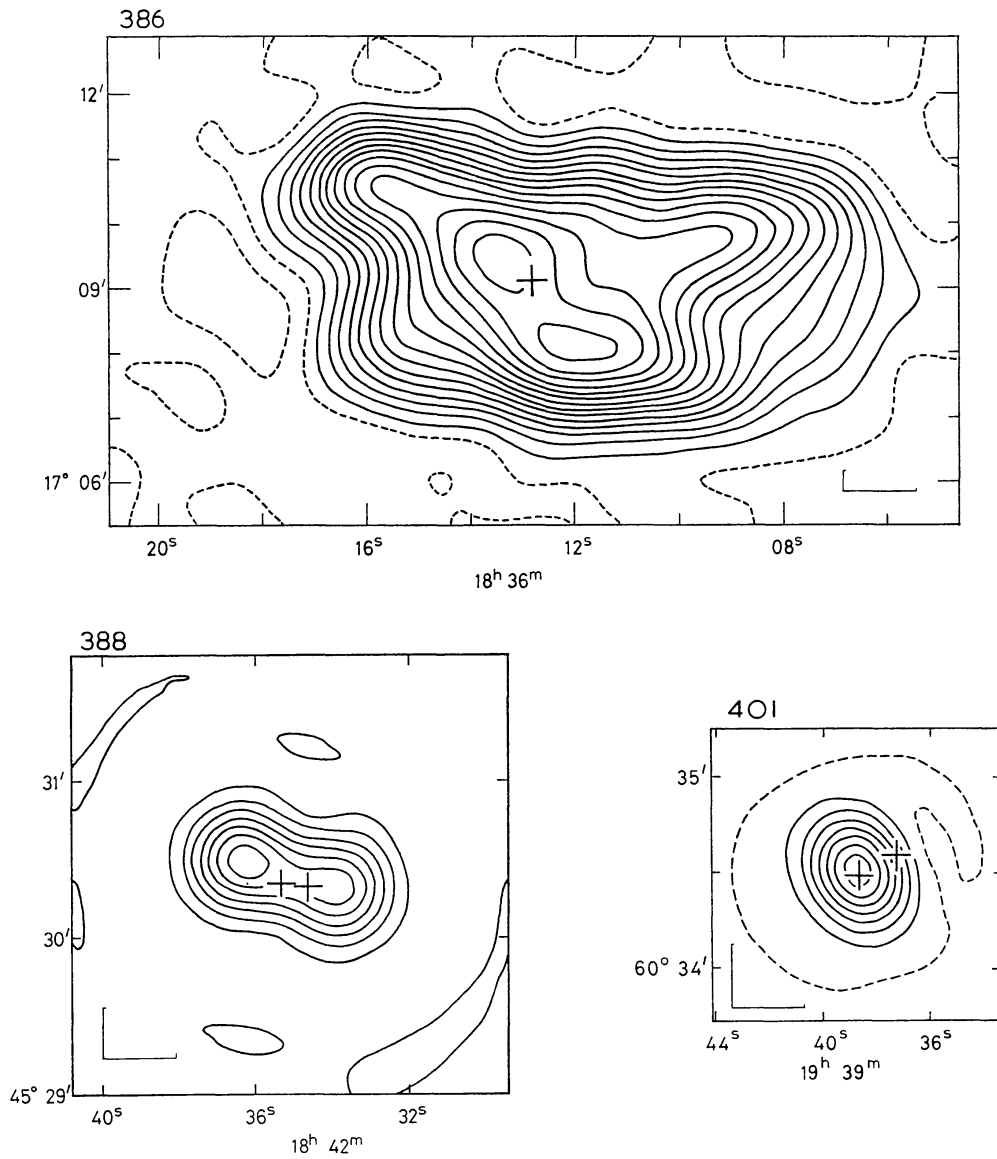
FIG. 16. *3C 386. The cross marks a* $13^m \cdot 0$ *object,* VV *3-47-10* (**35**), *probably the remnant of the supernova recorded in 1230 A.D. The redshift is* $0 \cdot 0008$ (**10**). *No change of source structure with frequency was detected.*

3C 388. The objects marked are a $14^m \cdot 5$ *galaxy, redshift* $0 \cdot 0917$, *plus a companion to the West (MMS, S).*

3C 401. The cross marks a red 19^m *galaxy with a faint companion to the North-West (W1).*
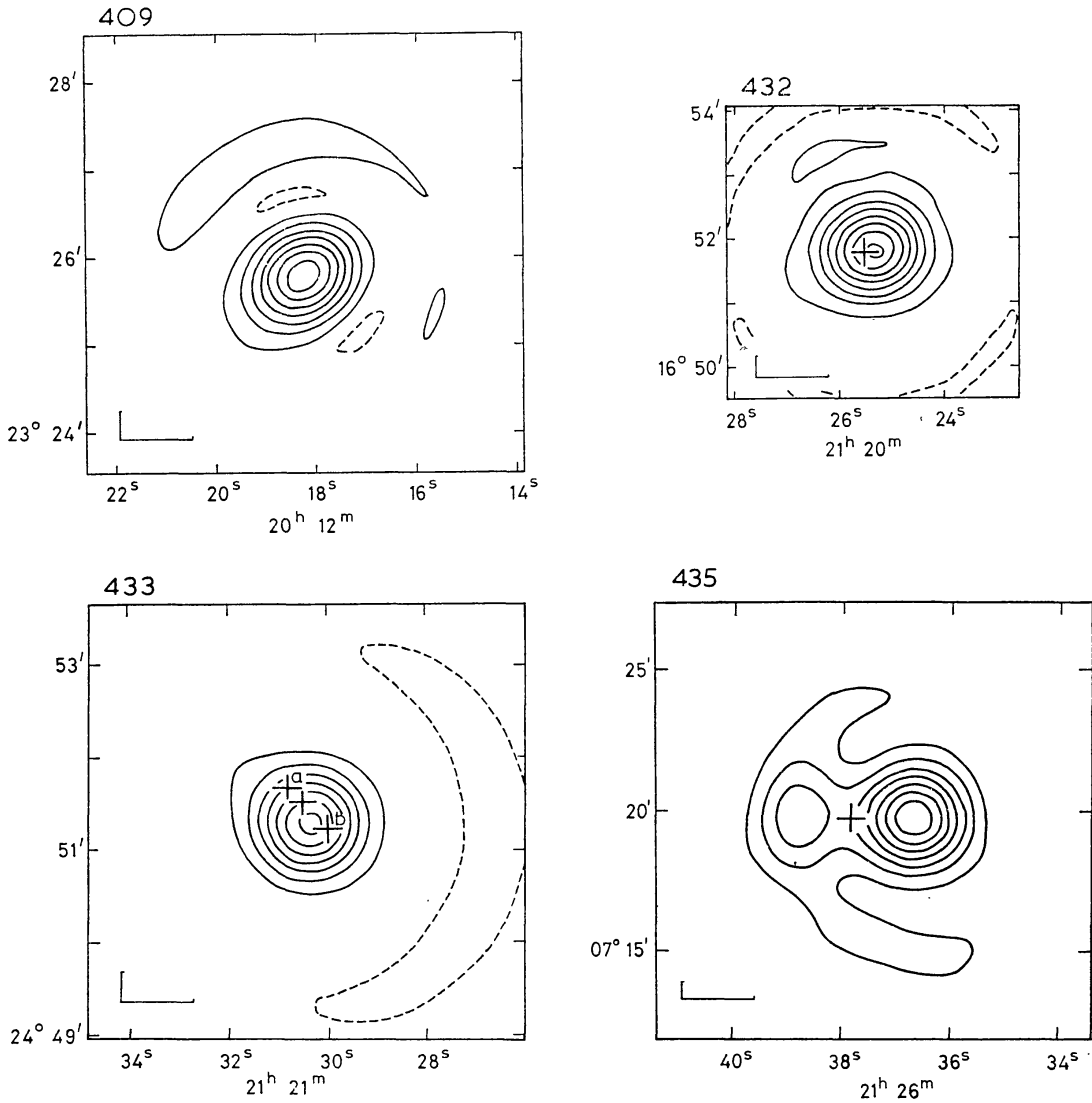
FIG. 17. 3C 409. *The optical field is obscured (W2).*

3C 432. *The cross marks a* $V = 17^m \cdot 96$ *QSS, with a redshift of* $1 \cdot 805$ *(W2, V)* (**31**).

3C 433. *There is a low brightness region of about 70″ arc total extent to the North-East of the main peak of this source which accounts for some 10 per cent of the flux at 1407 MHz. Objects marked are (a) Double galaxy* $16^m \cdot 0$. *(b) Red* 19^m *galaxy, possibly a cluster member (G, MMS, S). The redshift of the South-West galaxy of the double is* $0 \cdot 1025$ *(S).*

3C 435. *The object marked is a* $19^m \cdot 6$ *blue star (Schmidt, private communication to Wlerick & Véron* (**19**)*) probably unrelated* (**20**). *The field is otherwise blank.*

Field of 435·1

437

438
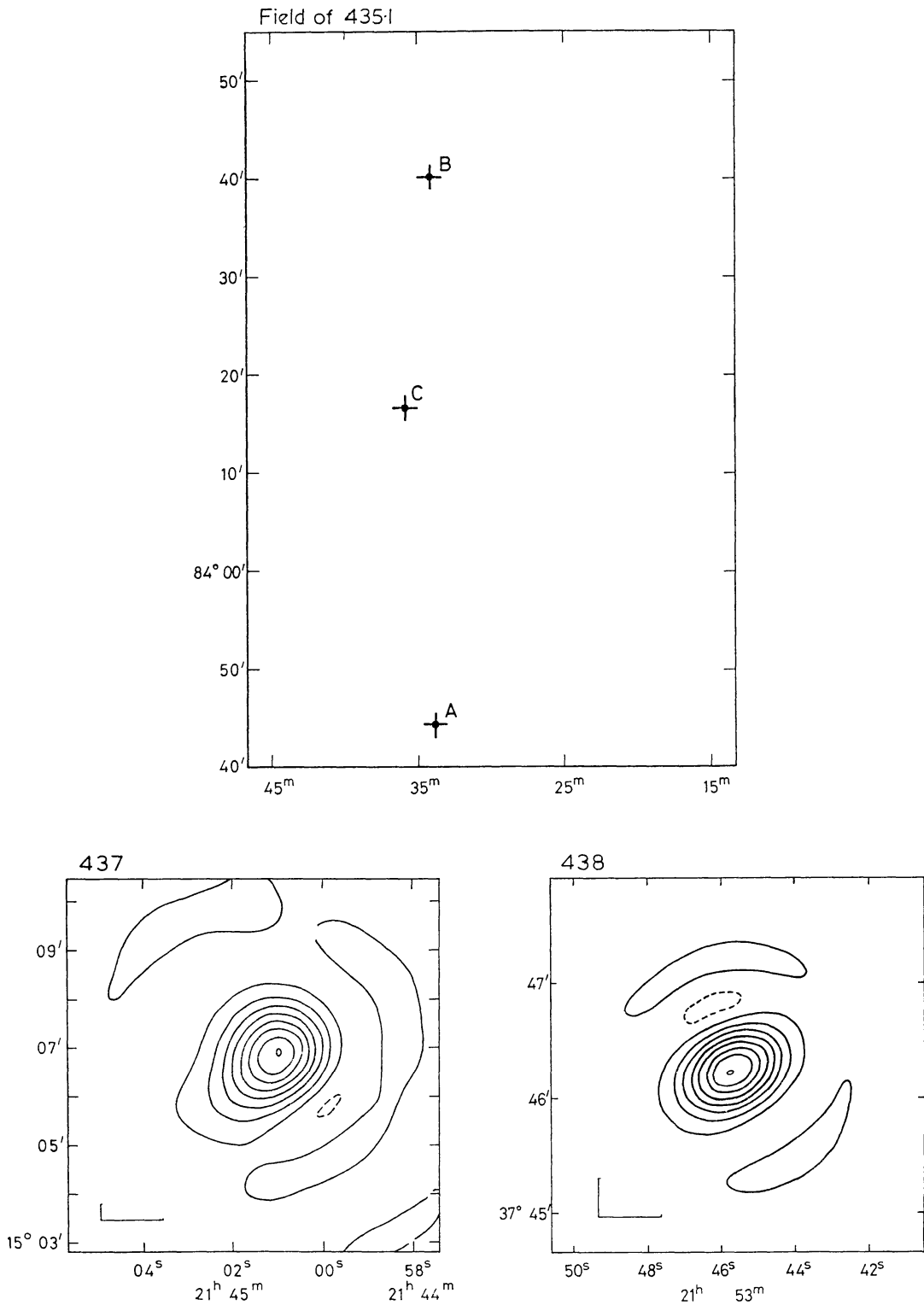
FIG. 18. 3C 435·1. *The crosses mark the positions of the three radio peaks of this source. Optically it is found that at (A) there is nothing within 30″ arc of the peak; in the field of (B) there is a cluster of galaxies at print limit and at (C) there may be a ~20^m very blue object about 7″ arc North of the peak. There is also a slightly blue 18^m galaxy ~40″ arc South-East of (C). The object suggested by Wyndham is a star* (36).

3C 437. *Nothing visible at the radio position* (W1).

3C 438. *There may be a diffuse red object near the radio position, only visible on the red print. Otherwise there is no object near the radio peak* (W1).
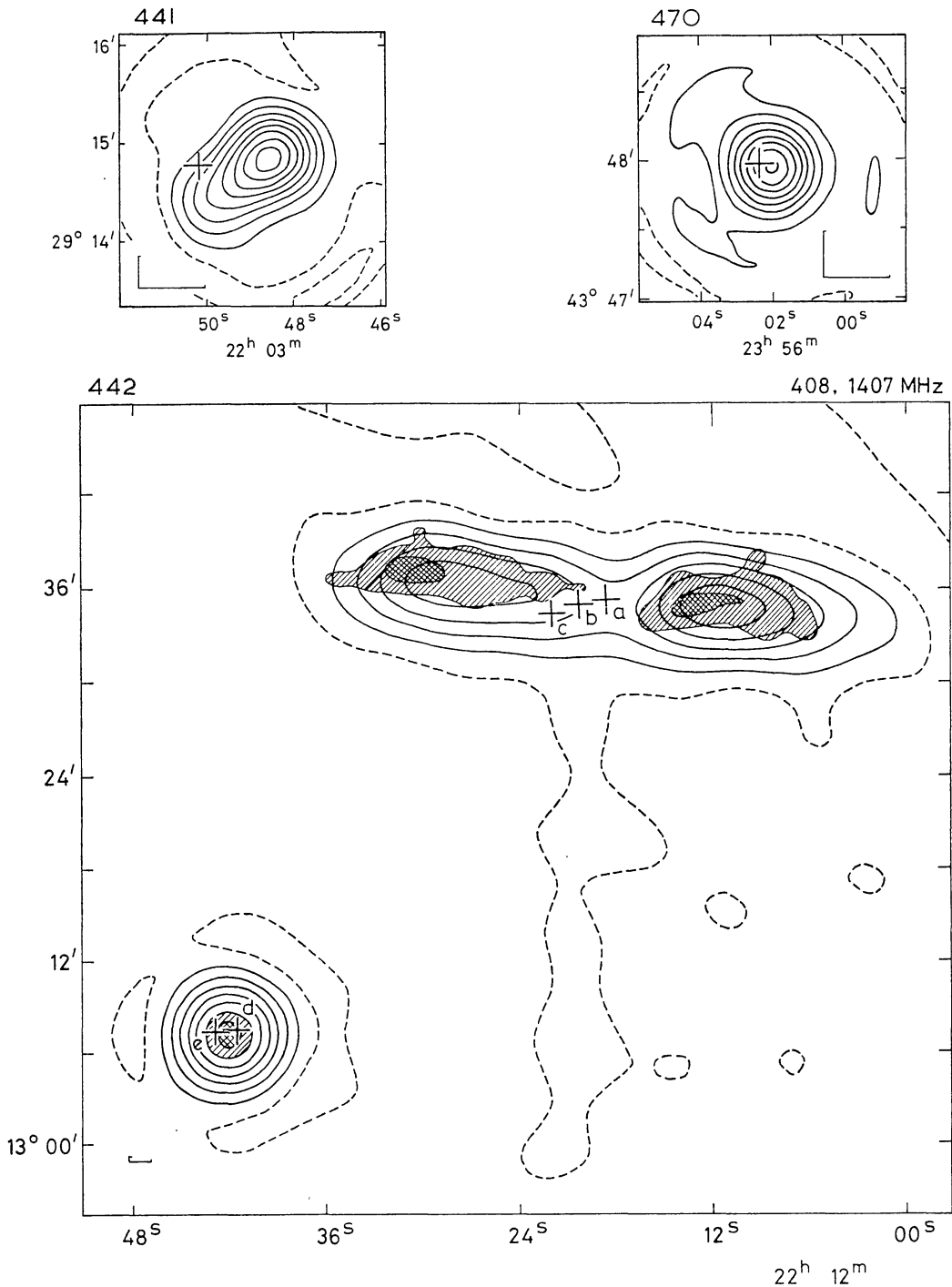
Fig. 19. 3C 441. *The cross marks a faint red stellar object. The field is otherwise empty near the radio position (W1).*

3C 470. *The object marked is a $19^m \cdot 5$ diffuse red galaxy (W2). There is a low brightness region of about $45''$ arc total extent to the North-East of the main peak, which accounts for some 25 per cent of the flux at 1407 MHz.*

3C 442. *The map shows the structure at 408 MHz, with that found at 1407 MHz superimposed as hatching. The brightest regions are cross-hatched. Because of the large extent of this source it was not possible to convolve the 1407 MHz map to the 408 MHz beam pattern completely. However, it was possible to show that the bridge of emission between the two well resolved components towards the North of the source has a steeper spectrum than the components it connects. The crosses mark (a) NGC 7236, a $13^m \cdot 8$ galaxy redshift = $0 \cdot 0262$ (10). (b) NGC 7237, a $14^m \cdot 5$ galaxy. (c) a $16^m \cdot 5$ galaxy, companion to NGC 7236/7 (37). The optical data on this field are discussed a length by Greenstein (38). In the field of the unresolved component to the South-East of the main source are (d) a red, $19^m \cdot 5$ galaxy, and (e) a very blue object at the limit of the red print.*
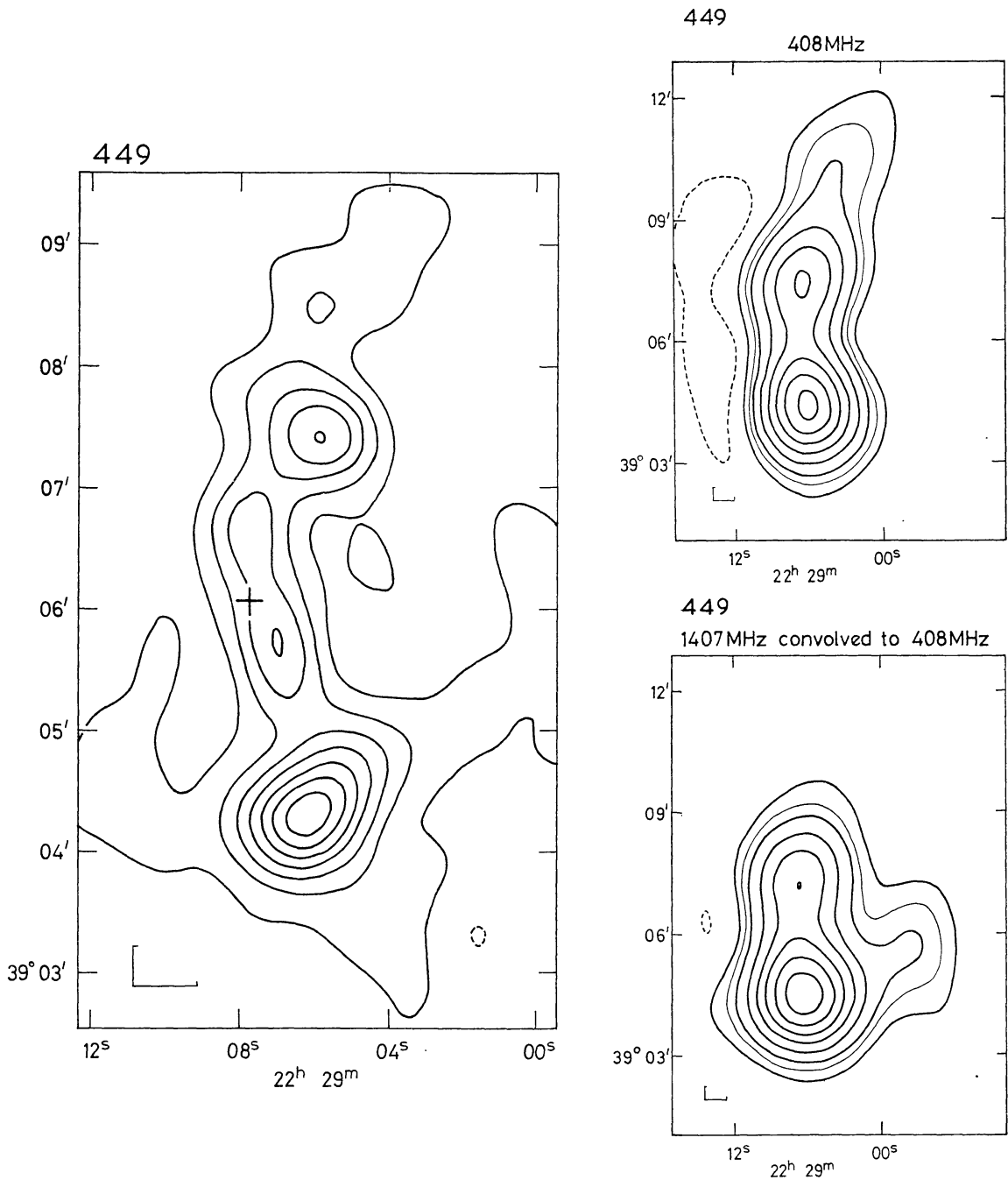
FIG. 20. 3C 449. *As the structure is appreciably different at each frequency three maps are given. The large map shows the structure found at 1407 MHz, and the other maps show the structure found at 408 MHz, and the 1407 MHz map convolved to the same beam pattern as used for the 408 MHz observations. These maps may be directly compared and it may be seen that there is a ridge of low surface brightness extending from the most southerly component of the radio source to the North-West which has a much flatter spectrum than the rest of the source, and that the extension present on the 408 MHz map is apparently absent at 1407 MHz and must show a very steep spectrum. The particularly wide range of spectral indices present in one source is most unusual. The field of this source contains a weak source which is resolved along the same line as the ridge from the most southerly component. It is at an angular distance of ~70' to the South-East of 3C 449. The cross on the 1407 MHz map marks the position of the brightest (12^m·5) galaxy (VV 6-49-29) (35) in a cluster in the field of the radio source. It has a redshift of 0·0181 (41).*

flux density of 3C 28 at each frequency. It is probably unrelated to 3C 28, and there is no obvious optical identification for this component.

3C 35. It is probable that some of the large scale structure of this source has been missed by the present observations.

3C 202. There is another radio peak (3C 201) about 70' to the North-West of the main peak probably not physically related to the central peak. Its flux density is 25 per cent of that of 3C 202 at 1407 MHz, and its peak is at $08^h 31^m 29^s \cdot 97 \pm 0^s \cdot 2$, $17° 29' 02'' \cdot 4 \pm 10''$.

3C 215. About 10 per cent of the flux density of this source probably comes from a large low brightness region with diameter about 50'' arc between half-power points.

3C 247. The observations of this source show that there are two faint sources 1^m to the west of 3C 247. They are separated by only 21'' in right ascension and each is slightly resolved at 1407 MHz. Their positions and flux densities are:

		Flux density ($\times 10^{-26}$ W m^{-2} Hz^{-1})	
R.A.	Dec.	1407 MHz	408 MHz
$10^h 55^m 10^s \cdot 06$	$43° 04' 51'' \cdot 4$	$0 \cdot 26$	$< 0 \cdot 35$
$10^h 55^m 12^s \cdot 00$	$43° 20' 47'' \cdot 9$	$0 \cdot 35$	$< 0 \cdot 35$

There is a faint red galaxy, $m_v \sim 20$, close to the position of the more southerly source, and no optical object within 30'' arc of the more northerly peak. The field between these sources was also examined, and a number of faint galaxies was found. Nothing, however, indicated that these sources might be physically related.

Fomalont (16) has reported an extensive 'halo' of emission for this source. The present observations, with additional measurements at interferometer baselines of 880λ and 220λ at 1407 MHz showed no evidence of this emission and set upper limits of $0 \cdot 1 \times 10^{-26}$ and $0 \cdot 7 \times 10^{-26}$ W m^{-2} Hz^{-1} at 1407 and 408 MHz to the flux density of any such extended component.

3C 386. This source is probably not a galaxy as had been suggested (10) but more likely the remnant of a supernova which was observed by Chinese astronomers in 1230 A.D. A detailed description of this source is now in course of preparation by the writer. There is a large low brightness region which accounts for about 15 per cent of the flux at 1407 MHz.

3C 435·1. The components of this source lie on one another's grating responses, so details of the structure are less reliable.

(c) *Change of source structure with frequency*

Sources with angular diameters greater than about 100'' arc are appreciably resolved at 408 MHz, and may be examined for change of source structure with frequency, i.e. a variation of spectral index across the source. Of the 14 such sources in the present sample, three (3C 35, 326, 442) have the map at one frequency too disturbed by grating responses either from the source itself or from nearby sources for a comparison to be possible. Of the remaining eleven sources, three (3C 223, 351 and 386) showed no change of structure, while eight showed some change of structure with frequency. Almost all the sources showed a rather complex structure at 1407 MHz, making it difficult to give more than a brief account of the change in structure. These are given in the figure captions. In the case of 3C 449, maps are also given at both frequencies.

In almost every case where change of structure with frequency was found, it was clear that components furthest from the associated optical object showed a steeper spectral index.

4. PHYSICAL PARAMETERS OF SOURCES OF KNOWN DISTANCE

Many of the radio sources present in this paper are believed to have reliable optical identifications, and, in many cases, the redshift of the optical object has been measured. It is assumed that the redshifts are cosmological in origin so that a distance may then be assigned to any of the latter objects. This has been done for the identified sources in Table II using an Einstein–de Sitter cosmology and a value of 100 km s⁻¹ Mpc⁻¹ for Hubble's constant. In the case of an object without a known redshift an approximate distance has been assigned on the assumption that the absolute visual magnitude of these objects, M_v, is $-21\cdot6$; there is no QSS without a redshift in this list. Some of the physical parameters which can then be derived are given in Table III. Physical parameters have not been given for sources whose identification is considered doubtful. The columns of Table III give:

(i) Source number. Several entries in the Table for one source indicate the separate components in the order listed in Table II.

(ii) Observed redshift z (if known).

(iii) Distance.

(iv) Overall linear size.

(v) The volume of the source or of the individual components; this has been computed on the assumption that the axis of the radio sources is perpendicular to the line of sight, and that the source is cylindrically symmetric about that axis. Because of projection effects these assumptions will usually underestimate the volumes of components which are extended along the radio axis.

(vi) The radio luminosity P in W Hz⁻¹ ster⁻¹ emitted at 1407 MHz.

(vii) An estimate of the minimum energy in the source assuming that the emission is due to synchrotron emission by relativistic particles, and that there is equipartition between the energies of the relativistic particles and of the magnetic field. It has been assumed that the protons have 100 times the energy of the electrons (**17**) and that the radio emission extends over the frequency range 10 to 10 000 MHz. The following formula has been used:

$$\text{Energy} = 2\cdot8 \times 10^{56}\, P^{4/7}\, 140^{4\alpha/7}\, V^{3/7} \left[\frac{0\cdot316 - 10^{(1-3\alpha)}}{2(2\alpha - 1)}\right]^{4/7} \text{ergs}$$

where P is in units of 10^{23} W Hz⁻¹ ster⁻¹ and V is the volume in units of 10^{66} cm³ (from Scheuer (**17**) with allowance for general α). The spectral indices used were obtained from the lists of Kellermann, Pauliny-Toth & Williams (**4**), rather than from the present observations. This is the only major difference between results given in I and those of the present paper.

(viii) The value of the corresponding magnetic field.

5. DISCUSSION

The present observations, together with those reported by Macdonald, Kenderdine & Neville (**2**), and those in preparation by Elsmore and Mackay, were

TABLE III

Source number	z	Distance (Mpc)	Size (kpc)	Volume (10^{66} cm³)	P_{1407} (10^{23} mks)	Minimum energy (10^{57} erg)	H (10^{-5} gauss)
3C 28	0·1959	510	60	<730	49	<380	>7·4
35		147	380	1500	4·8	62	2·1
42		870	77	<2500	420	<1100	>6·9
98	0·0306	90	130	150	4·0	18	3·5
				71	4·5	14	4·6
123		780	83	1300	4800	3100	16
132		610	38	<990	190	<490	>7·2
175	0·768	1490	195	<28000	690	<5600	>4·6
				<28000	1000	<7000	>5·1
192	0·0596	171	163	<57	5·2	<13	>4·9
				190	3·5	17	3·1
				780	6·5	58	2·8
194		870	52	<750	260	<550	>8·7
204	1·112	1870	137	<720	1000	<1500	>15
				<720	850	<1400	>14
205	1·534	2230	72	<2000	6900	<5800	>18
212		700	145	<2100	160	<590	>5·4
				2100	18	170	2·9
215	0·411	950	120	<9600	270	<2000	>4·7
223	0·1367	372	462	250	33	82	5·8
				690	25	110	4·0
226		780	97	<8900	230	<1900	>4·7
228		870	136	<2400	470	<1100	>7·0
249·1	0·3107	760	70	820	210	420	7·3
254	0·734	1440	56	<2100	1800	<3100	>12
265		870	207	<1900	140	<810	>6·7
				<1200	240	<920	>9·1
277·2		780	122	<2600	130	<660	>5·2
				2200	67	410	4·5
277·3	0·0857	242	31	220	15	44	4·6
293	0·0452	131	48	9·7	0·58	1·9	4·5
				9·7	0·41	1·7	4·3
				<9·7	7·5	<9·0	>9·8
310	0·0543	157	179	17000	19	980	2·5
314·1		280	221	1900	2·4	78	2·1
				4800	10	270	2·4
315	0·1086	301	66	6600	39	440	2·6
320		545	37	<590	72	<270	>6·8
336	0·927	1680	118	<7000	2900	<6000	>9·4
351	0·371	876	182	1300	46	200	4·0
				<480	370	<440	>9·7
388	0·0917	258	30	140	21	61	6·7
				<60	24	<46	>9·0
401		700	42	<440	390	<550	>11
432	1·805	2420	50	<8100	7000	<14000	>13
433	0·1025	279	64	270	98	200	8·7
442	0·0262	77	98	<1300	0·84	<34	>1·7
				<1600	0·90	<40	>1·6
449	0·0181	54	76	0·83	0·034	0·12	3·8
				0·72	0·16	0·26	6·2
				1·9	0·37	0·65	5·9
				<0·77	0·093	<0·20	>5·2
				<0·77	0·054	<0·15	>4·4
470		780	34	<520	220	<490	>9·9

made to obtain data for a complete sample of radio sources from the revised 3C catalogue, which would provide a basis for a number of theoretical investigations.

While the radio survey is complete for all 200 sources with $S_{178} \geqslant 9 \times 10^{-26}$ W m^{-2} Hz^{-1}, $\delta > +10°$, $|b^{II}| > 10°$, no attempt has yet been made to observe the corresponding regions of the optical sky in a similarly complete manner, with the exception of the National Geographic–Palomar Sky Survey. As a result, the optical identification work for this sample of radio sources is incomplete in a number of important ways. Regions of sky which are obscured are unlikely to yield identifications in the foreseeable future, and these will not be included in the following discussion.

The most complete 3C identification programme has been carried out by Wyndham (**8, 9**) using both the prints and plates of the National Geographic–Palomar Sky Survey with radio positions whose accuracy was ± 12″ arc in each coordinate. In the majority of cases, observations of the present sample at Cambridge have confirmed these identifications, but it has also been possible to describe in detail the important selection effects operating on the identifications.

(1) Limiting magnitudes for the Sky Survey Prints are approximately 20 m$_R$ (red) and 21 m$_{pg}$ (blue) (**18**). For more compact sources where the prints are of the highest quality, it is possible to approach these limits for the purposes of identification. In general identifications may be be made down to a level about one magnitude brighter than this for compact sources, where the radio position is known to within a few seconds of arc in each coordinate. For more extensive sources, the magnitude limit for an ' acceptable ' identification is brighter than this because of the correspondingly larger area within which a related object might lie. This has not meant, however, that the most extensive sources are usually unidentified, because for many of these sources the optical field is dominated by a bright (11^m–16^m) object, which is usually taken to be the identification. Thus the limiting magnitude is not simply determined by the quality of the photographic plates, but also by the angular area covered by the radio source to be identified. Extensive sources of low brightness are less likely to be identified than more compact, brighter sources.

(2) Identifications with optical objects which are close to the print limits are complicated by the fact that a particular clump of silver grains might be a print or plate defect. If such an object appears on both red and blue prints, then it is almost certainly not a defect, and clearly a possible identification. There is therefore a selection effect operating in favour of identifications being made with an object of neutral colour (equally bright on red and blue prints). This effect may be eliminated if duplicate plates are available.

(3) The suggested identification may be the result of a purely chance coincidence. This possibility has been discussed by Wyndham (**9**).

(4) An identification is taken as confirmed if a measurement of its redshift shows it to be receding from us with a large apparent velocity. Suggested identifications found to be local are usually discarded. Accurate positions for a large number of unresolved or slightly resolved sources show a very strong correlation between the positions of compact radio sources and objects with large redshift ($z > 0.1$). Further, while there is no evidence to suggest that identifications of some sources ought to be made with galactic stars (**19, 20**), selection against local objects is certainly present. One source in the present sample, 3C 386, hitherto believed to be extragalactic, is, in fact, probably within our own galaxy. Another, 3C 326 may be

related to the North Galactic spur, and not associated with the large cluster of galaxies found by Wyndham (9).

(5) While it is normally assumed that a source is properly identified once one object with an appreciable redshift has been found, it often happens that the identified object, if it is a galaxy, is within a cluster of fainter galaxies. In some cases faint clusters of galaxies are found near the radio positions of compact sources, and for larger sources, other galaxies, probably cluster members, are found in parts of the radio source well separated from the central galaxy (9). It is becoming increasingly clear that a number of sources hitherto identified with a single bright galaxy, or even left unidentified, could be satisfactorily identified with a cluster of galaxies.

Despite the selection effects mentioned above, there should now be enough data available to allow some considerable progress towards a detailed understanding of the structure and evolution of extra-galactic radio sources.

Mullard Radio Astronomy Observatory, Cavendish Laboratory, Cambridge.

REFERENCES

(1) Elsmore, B., Kenderdine, S. & Ryle, M., 1966. *Mon. Not. R. astr. Soc.*, **134**, 87.
(2) Macdonald, G. H., Kenderdine, S. & Neville, A. C., 1968. *Mon. Not. R. astr. Soc.*, **138**, 259.
(3) Longair, M. S. & Macdonald, G. H., 1969. *Mon. Not. R. astr. Soc.*, **145**, 309.
(4) Kellermann, K. I., Pauliny–Toth, I. I. K. & Williams, P. J. S., 1969. *Astrophys. J.*, **157**, 1.
(5) Griffin, R. F., 1963. *Astr. J.*, **68**, 421.
(6) Véron, P., 1966. *Astrophys. J.*, **144**, 861.
(7) Longair, M. S., 1965. *Mon. Not. R. astr. Soc.*, **129**, 419.
(8) Wyndham, J. D., 1965. *Astr. J.*, **70**, 384.
(9) Wyndham, J. D., 1966. *Astrophys. J.*, **144**, 459.
(10) Matthews, T. A., Morgan, W. W. & Schmidt, M., 1964. *Astrophys. J.*, **140**, 35.
(11) Schmidt, M., 1965. *Astrophys. J.*, **141**, 1.
(12) Sandage, A. R., Véron, P. & Wyndham, J. D., 1965. *Astrophys. J.*, **142**, 1307.
(13) Wills, D. & Parker, E. A., 1966. *Mon. Not. R. astr. Soc.*, **131**, 503.
(14) Edge, D. O., Shakeshaft, J. R., McAdam, W. B., Baldwin, J. E. & Archer, S., 1959. *Mem. R. astr. Soc.*, **68**, 37.
(15) Bennett, A. S., 1962. *Mem. R. astr. Soc.*, **68**, 163.
(16) Fomalont, E. B., 1968. *Astrophys. J. Suppl. Ser.*, **15**, 203.
(17) Scheuer, P. A. G., 1968. Summer School, Plasma Astrophysics, Varenna.
(18) Minkowski, R. L. & Abell, G. O., 1963. Stars and Stellar Systems, Vol. 3. Appendix II. University of Chicago Press.
(19) Wlerick, G. & Véron, P., 1967. *Ann. Astrophys.*, **30**, 341.

(20) Mackay, C. D., 1967. *Nature*, **216**, 1091.
(21) Taylor, J. H. & de Jong, J. L., 1968. *Astrophys. J.*, **151**, 33.
(22) Adgie, R. L. & Gent, H., 1966. *Nature*, **209**, 549.
(23) Maltby, P., Matthews, T. A. & Moffet, A. T., 1963. *Astrophys. J.*, **137**, 153.
(24) de Jong, M. L., 1967. *Astrophys. J.*, **148**, 651.
(25) Taylor, J. H., 1966. *Astrophys. J.*, **146**, 646.
(26) Lynds, C. R., 1967. *Astrophys. J.*, **147**, 837.
(27) Sandage, A. R., 1966. *Astrophys. J.*, **145**, 1.
(28) Hazard, C., Mackey, M. B. & Nicholson, W., 1964. *Nature*, **202**, 227.
(29) Lynds, C. R., Hill, S. J., Heare, K. & Stockton, A. N., 1966. *Astrophys. J.*, **144**, 1244.
(30) Anderson, B. L. *et al.*, 1965. *Nature*, **205**, 375.
(31) Schmidt, M., 1966. *Astrophys. J.*, **144**, 443.
(32) Schmidt, M., 1965. *Astrophys. J.*, **141**, 1295.
(33) Adgie, R. L., 1964. *Nature*, **204**, 1028.
(34) Clark, B. G. & Hogg, D. E., 1966. *Astrophys. J.*, **145**, 21.
(35) Vorontsov–Velyaminov, B. A., 1959. Atlas and Catalogue of interacting galaxies.
(36) Burbidge, G. & Burbidge, E. M., 1967. *Quasi-stellar objects*, W. H. Freeman & Co., San Francisco & London.
(37) Bolton, J. G., 1960. Observations of the Owens Valley Radio Observatory, No. 5.
(38) Greenstein, J. L., 1962. *Astrophys. J.*, **135**, 679.
(39) Sandage, A. R., 1965. *Astrophys. J.*, **141**, 1560.
(40) Pskovskii, Y. I., 1965. *Soviet Astr.*, **9**, 526.
(41) Sandage, A. R., 1967. *Astrophys. J.*, **150**, L 145.

5